Investigation of the role of Hsp70 in the uptake of Granzyme B by malaria parasite-infected erythrocytes

A thesis submitted in fulfilment of the requirements for the degree of

MASTER OF SCIENCE IN BIOCHEMISTRY

SCHOOL OF MATHEMATICS AND NATURAL SCIENCE

DEPARTMENT OF BIOCHEMISTRY

UNIVERSITY OF VENDA

by

RAMATSUI LEBOGANG

11640992

Supervisor: Prof. A. Shonhai

Co-supervisor: Dr. T. Zininga

February 2019

ABSTRACT

In 2017 malaria cases were estimated at 219 million and of these 435 000 resulted in death. Malaria is transmitted by female Anopheles mosquitoes which thrive in tropical and sub-tropical areas. Malaria is caused by five species from the genus *Plasmodium*, namely *P. falciparum*, *P. vivax*, *P. ovale*, *P. malariae and P. knowlesi*. *P. falciparum* causes the most severe form of the disease. *P. falciparum* has a complex life cycle in the human and mosquito hosts exposing the parasite to environmental changes, resulting in upregulation of heat shock proteins (Hsps). These Hsps facilitate protein folding and protein disaggregation. Hsp70 is a molecular chaperone whose function is to facilitate protein folding. *P. falciparum* Hsp70-x is the only member of this family of proteins that is exported to the erythrocyte cytosol by the parasite. PfHsp70-x has been implicated in the development of malaria pathogenesis. This is largely due to its association with *P. falciparum* erythrocyte membrane protein 1 (PfEMP1), an important virulent factor that is exposed to the exterior of the infected erythrocyte. In tumour cells, cell surface- bound Hsp70 is known to sensitize the tumour cells to cytolytic attack that is mediated by NK cells. Cell surface bound Hsp70 is thought to recruit NK cells and Granzyme B (GrB) via its 14 amino acid sequence, TKDNNLLGRFELSG, known as the TKD motif. Both PfHsp70-x and human Hsp70 (hHsp70) contain the TKD motif. Thus, this study sought to investigate the role of Hsp70 in facilitating the selective targeting of malaria parasite-infected erythrocytes by GrB. To this end, recombinant hHsp70 and PfHsp70-x were successfully expressed in *E. coli* and purified. Using slot blot and ELISA, it was observed that both PfHsp70-x and hHsp70 directly interact with GrB. PfHsp70-x showed greater affinity for GrB than hHsp70. In addition, using parasites cultured at the erythrocyte stage it was noted that GrB exhibits potent antiplasmodial activity (IC50 of 0.5µM). In addition, the findings suggest that GrB interacts with both Hsp70s (of parasite and human origin) resident in the infected erythrocyte. This makes GrB a promising antimalarial agent.

Key words: Malaria, *Plasmodium falciparum*, Heat shock proteins, PfHsp70-x, Granzyme B

Declaration

I, Lebogang Ramatsui, declare that this thesis submitted by me to the University of Venda for the Master of Science degree in Biochemistry has not been submitted to any other University. This is my work with exception of referenced material which has been cited in text and acknowledged.

Signature……..….. Date…….

Dedication

This thesis is dedicated to my mother (Mosibudi Lydia Ramatsui), my sister (Katlego) and my two nieces (Mosibudi and Lebogang).

Acknowledgements

I thank God for the strength and resilience to complete this study. I am grateful for the patience, guidance, expertise and mentorship provided by my supervisor Prof. Addmore Shonhai during the entire duration of the project. His support and encouragement were key to the completion of this project.

I also would like to extend my gratitude to my co-supervisor Dr. Tawanda Zininga for his mentorship, guidance, patience and support.

I wish to acknowledge the following people for work done:

- Prof. Gabriele Multhoff (School of Medicine, Technical University of Munich, Germany) for production of Human Gramzyme B.
- Dr. Heinrich Hoppe (Department of Microbiology and Biochemistry, Rhodes University, South Africa) for *Plasmodium falciparum* 3D7 cell culture.

I wish to extend acknowledgement to the National Research Foundation (NRF South Africa) for funding this research project.

Lastly, I am grateful for the ProBioM research group and the department of Biochemistry for their moral support throughout this study.

Outputs

Peer Reviewed Publications:

Zininga, T., **Ramatsui, L.**, Shonhai, A. (2018). Heat Shock Proteins as Immunomodulants. Molecules. 23: 2846.

Mabate, B., Zininga, T., **Ramatsui, L.**, Makumire, S., Achilinou, I., Dirr, H., Shonhai, A. (2018). Structural and biochemical characterization of *Plasmodium falciparum* Hsp70-x reveals functional versatility of its C-terminal EEVN motif. Proteins: Structure Function and Bioinformatics. 86: 1189-1201.

Zininga, T., **Ramatsui, L.**, Makhado, P., Makumire, S., Achilinou, I., Hoppe, H., Dirr, H., Shonhai, A. (2017). (−)-Epigallocatechin-3-gallate inhibits the chaperone activity of *Plasmodium falciparum* Hsp70 chaperones and abrogates their association with functional partners. Molecules. 22: 2139.

Zininga, T., Pooe, O., Makhado, P., **Ramatsui, L.**, Prinsloo, E., Achilonu, I., Dirr H., Shonhai, A. (2017). Polymyxin B inhibits the chaperone activity of *Plasmodium falciparum* Hsp70. Cell Stress and Chaperones. 22: 707-715.

Conference Presentations:

Ramatsui, L., Zininga, T., Achilonu, I, Prinsloo, E., Hoppe, H., Dirr, H., Shonhai, A. Investigation of the role of Hsp70 in Granzyme B-mediated in malaria therapy. Parasitological Society of South Africa Conference. 16 -18 September 2018. Tshipise Resorts (South Africa).

Zininga, T., **Ramatsui, L.**, Shonhai, A. Investigation of the role of Hsp70 in Granzyme B-mediated in malaria therapy. Biophysics and Structural Biology at Synchrotrons Workshop. 16 -24 January 2019, University of Cape Town (South Africa).

Table of contents

List of Figures

List of Tables

1. Introduction and literature review

1.1. Background

Malaria is a protozoan disease responsible for an estimated 219 million reported cases in 2017 which resulted in 435 000 deaths (WHO, 2018). The sub-Saharan region accounted for 92% of malaria cases and deaths in 2017 (WHO, 2018). The optimal conditions for growth and development of the female *Anopheles* mosquito vector are in the tropical and sub-tropical areas (CDC, 2016; WHO, 2018). Human malaria is caused by five species from the *Plasmodium* genus, namely *P. falciparum*, *P. vivax*, *P. ovale*, *P. malariae* and *P. knowlesi* (WHO, 2018). *P. falciparum* is the most dominant malaria parasite in sub-Saharan Africa, accounting for 98% of estimated malaria cases in 2017 (WHO, 2018).

1.2. *P. falciparum* life cycle

P. falciparum undergoes a complex life cycle that traverses both the human host and the mosquito vector (Cox, 2010). The life cycle begins when an infected female *Anopheles* mosquito takes a blood meal and injects infective sporozoites into the peripheral blood circulatory system (Figure 1.1; Boyle *et al*., 2010). The sporozoites find their way to the liver where they invade hepatocytes (Bozdech *et al*., 2003). In the liver the sporozoites start dividing and mature into schizonts. The schizonts then rupture and release merozoites which invade erythrocytes (Morrissette and Sibley, 2002; Eaton *et al*., 2012). Once in the erythrocyte, the merozoites develop into the ring stage that evolves into a trophozoite (Bannister, 2001). The trophozoites further develop into mature schizonts (merozoites) (Bannister, 2001). The infected erythrocytes then rupture releasing the merozoites into the blood stream to invade other erythrocytes (Boyle *et al*., 2010). A subset of the merozoites differentiate into microgametes (male) and macrogametes (female) during the process known as gametogenesis (Rowe *et al*., 2009; Boyle *et al*., 2010). The gametocytes are ingested by the mosquito vector when it takes a blood meal. The flagellated microgamete fertilizes a macrogamete forming a zygote in the mosquito gut (Billker *et al*., 1997). The zygote, after the fusion of nuclei during fertilization develops into the ookinete which penetrates the mosquito gut epithelium and develops into an oocyst. Inside the oocyst, the ookinete nucleus divides to produce thousands of sporozoites (sporogony) (Boyle *et al*., 2010).

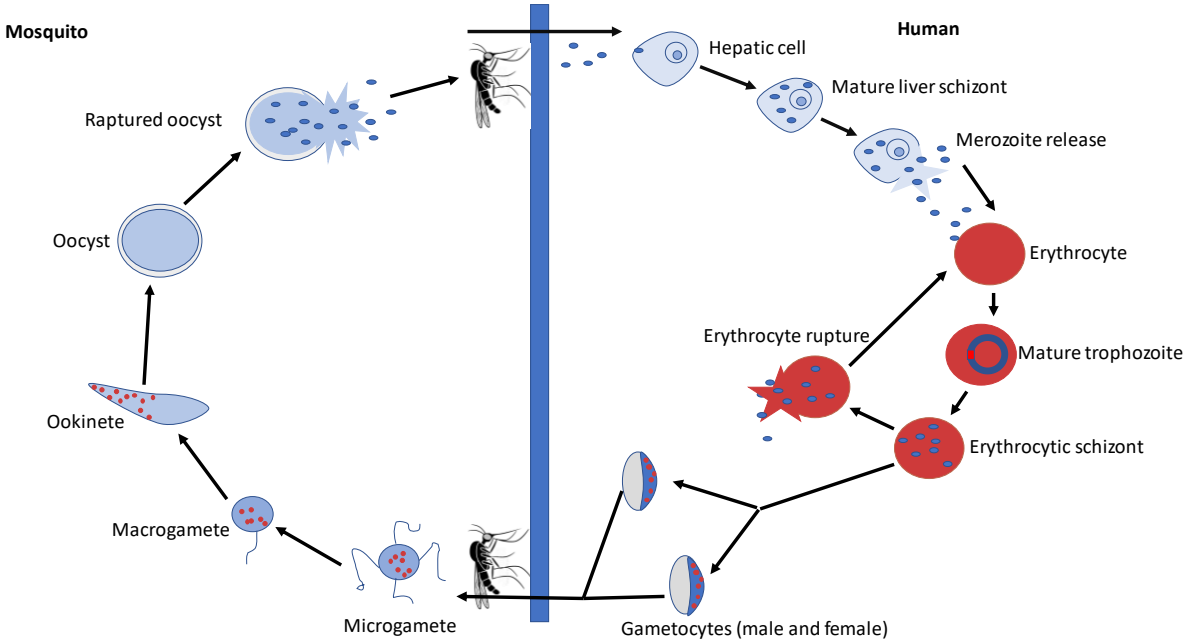

Figure 1.1. Schematic representation of the life cycle of *P. falciparum*
The parasite undergoes various parasite developmental stages in the host and the vector (adapted from Rowe *et al.*, 2009).

The oocyst ruptures releasing sporozoites which find their way to the mosquito salivary glands (Crompton *et al.*, 2010). The sporozoites then mature and are injected in the next victim (host) when a mosquito takes a blood meal, resulting in the spread of malaria. Most of the malaria treatment options target the symptomatic erythrocytic stages of the malaria life cycle.

1.3. Treatment of malaria

The majority of antimalarial drugs are aimed at rapidly eliminating the erythrocytic stages of the malaria parasites (Cui *et al.*, 2015; WHO, 2016). Chloroquine was the most widely used drug for the treatment of uncomplicated malaria for several years (Cui *et al.*, 2015). Chloroquine is a 4-aminoquinoline derivative of quinine which is thought to interfere with hemoglobin digestion by binding to hematin. The binding of chloroquine to hematin prevents its incorporation into the hemozoin crystal (Thomé *et al.*, 2013). The hematin interferes with the parasite detoxification processes, resulting in damage to parasite cell membranes by lipid peroxidation mechanism (Thomé *et al.*, 2013; Cui *et al.*, 2015). Chloroquine has lost its efficacy due to the spread of resistant malaria parasites. This has resulted in the alternative use of drugs such as pyrimethamine/sulfadoxine (Fansidar), amodiaquine or mefloquine as first line antimalarial drugs in areas of chloroquine resistance (WHO, 2016). These drugs have since been replaced by artemisinin-based combination therapy (ACT) due to increased resistance to mono-therapy by the *P. falciparum* parasite (WHO, 2016). ACT is made up of a potent

artemisinin component, which rapidly clears most parasites, coupled to a longer acting partner drug, which eliminates remaining parasites to reduce resistance (Cui *et al*., 2015). Artemisinins act by generating carbon-centered free radicals or reactive oxygen species (ROS), which readily react with free hemin resulting in formation of heme–artemisinin adducts (Cui and Su, 2009). Heme–artemisinin adducts interact with the *P. falciparum* histidine-rich protein II (PfHRP II), which displaces the heme from PfHRP II causing inhibition of heme polymerization and hemozoin formation (Cui and Su, 2009). ACTs are very effective and have a high tolerance (Cui *et al*., 2015). However, high treatment failure rates with ACTs due to development of resistance were reported in the Greater Mekong Subregion (GMS) (India, Thailand, Vietnam) (WHO, 2018).

1.4. Antimalarial drug resistance

The effectiveness of antimalarial drug has been reduced due to emerging drug resistant parasite strains (WHO, 2015). *P. falciparum* is commonly associated with resistance to antimalarial drugs (WHO, 2016). The resistance is a result of delayed clearance of parasites from the host's blood circulation during treatment with antimalarial drugs (WHO, 2016). There are multiple mechanisms for resistance to antimalarial drugs depending on the drug. *P. falciparum* multi-drug resistance gene 1 (*Pfmdr-1*) has been associated with resistance to multiple drugs, due to single nucleotide polymorphisms (SNPs) (Cui *et al*., 2015). Resistance to amodiaquine has been linked with SNPs which result in an amino acid change in codons 86 (N86Y), 184 (Y184F), and 1246 (D1246Y) on *Pfmdr-1* (Thomsen, 2011). Chloroquine resistance is linked to multiple mutations in *P. falciparum* chloroquine resistance transporter (*PfCRT*) (Wellems and Plowe, 2001; Thomsen, 2011). *P. falciparum* has also shown resistance to antifolates such as pyrimethamine which is often used in combination with sulfadoxine (SP). This is a result of point mutation in the dihydrofolate reductase (*dhfr*) gene which targets the dihydrofolate reductase enzyme (Cui *et al*., 2015). Mutations at codon 51 (N51I) and 59 (C59R) of the *dhfr* gene result in resistance to pyrimethamine (Gregson and Plowe, 2005). Pyrimethamine acts by binding to and inhibiting dihydrofolate reductase (DHFR) which plays an essential role in parasite growth (Gregson and Plowe, 2005). Pyrimethamine resistant parasites contain the altered DHFR that exhibits reduced affinity for the inhibitor (Gregson and Plowe, 2005). Slow parasite clearance rates after treatment with artemisinin derivatives is associated with 20 mutations in *kelch13* affecting the encoded propeller and Broad-Complex, tramtrack and Bric a brac (BTB)/Poxvirus and Zinc finger (POZ) domains (Miotto *et al.*, 2015). In addition, artemisinin resistance in *P. falciparum* is also linked with polymorphisms in *mdr2* (multidrug

resistance protein 2) and *crt* (chloroquine resistance transporter) (Miotto *et al*., 2015). The *P. falciparum* resistance to artemisinin is an urgent public health concern. The ability of the parasite to survive under drug pressure is in part due to the upregulation of heat shock proteins (Hsps) making Hsps potential drug targets (Banerji, 2009; Evans *et al*., 2010).

1.5. Export of parasite proteins

P. falciparum infects erythrocytes and causes changes in the biochemical and structural properties of the host cell (Maier *et al*., 2008). The changes are a result of exported parasite proteins to the erythrocyte cytosol (Külzer *et al*., 2012). In the erythrocyte, the parasite develops enveloped by the parasitophorous vacuole (PV) (Figure 1.2).

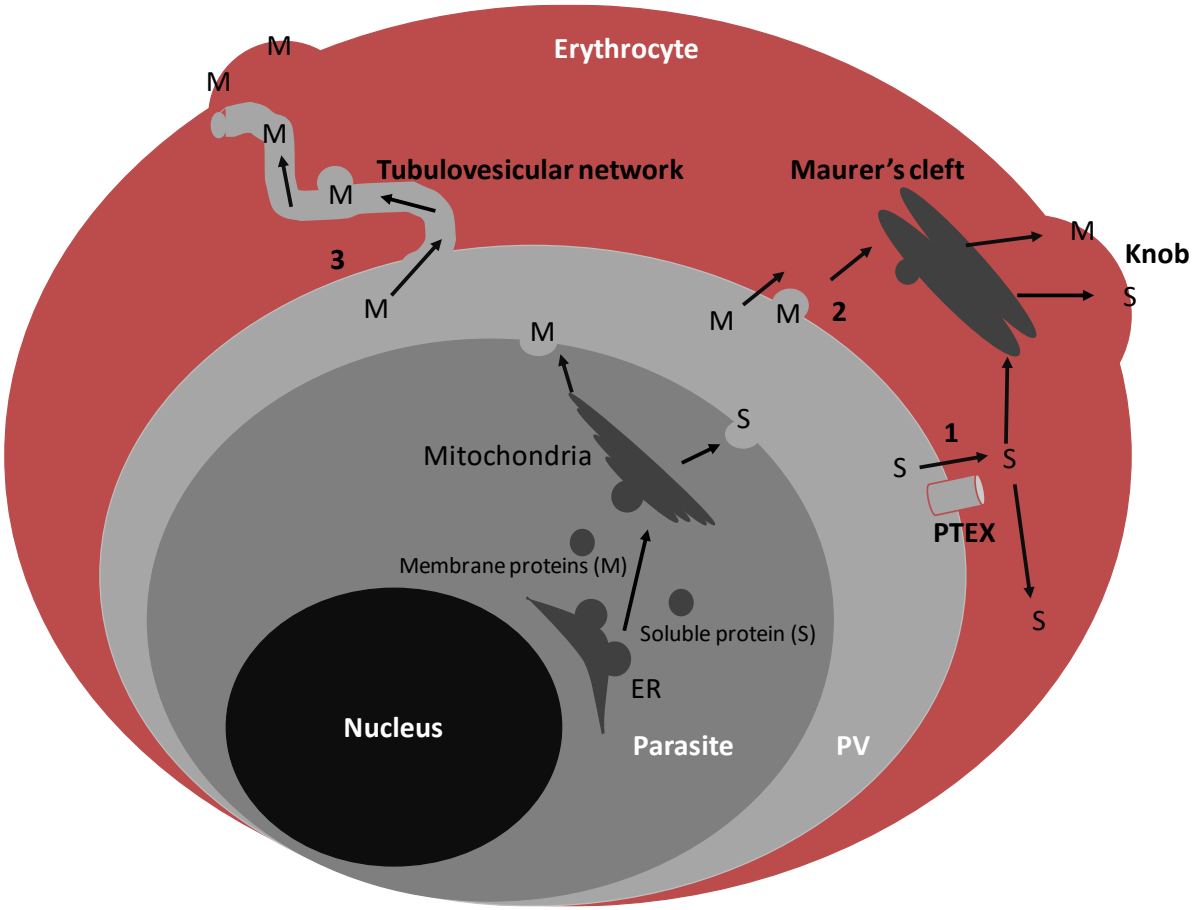

Figure 1.2. Illustration of the potential export mechanisms of parasite proteins
(1) Soluble proteins 'S' are potentially shuttled across the PV membrane into the erythrocyte cytosol through an ATP dependent translocon system 'PTEX'. (2) Membrane proteins 'M' are thought to be trafficked to the erythrocyte via a vesicular-based transport system to the Maurer's clefts and subsequently to the erythrocyte membrane where they may associate with the cytoadherence complex in the knob structures. (3) Membrane proteins may also traverse a tubulovesicular network (TVN) branched from the PV, to reach the erythrocyte membrane (Adapted from Botha *et al*, 2007).

For parasite synthesized proteins to be exported to the host cytosol they must pass through both the parasite plasma membrane and the PV membrane (Cobb *et al*., 2017). Transport across the

parasite membrane occurs through the default secretory pathway, then via the translocon complex within the PVM (Botha *et al*., 2007). Proteins exported beyond the PVM require the presence of the export motif called the *Plasmodium* export element (PEXEL) or vacuolar translocation signal (VTS) (Boddey *et al.*, 2009). The motif is conserved in *Plasmodium* species and contains a pentameric sequence R/QnLnE/Q/D, where n is any non-charged amino acid (Chang *et al.*, 2008; Boddey *et al.*, 2009). As a prerequisite for export, proteins containing the PEXEL motif undergo processing in the ER (Sijwali and Rosenthal, 2010). Upstream of the PEXEL motif there's a hydrophobic transmembrane domain that functions as a signal sequence which allows co- or post-translational insertion of PEXEL containing proteins into the ER (Crabb *et al.*, 2010). The PEXEL motif is cleaved by the pexelase protease in the ER leaving the exported protein capped with xE/Q/D at the N-terminus, which is later acetylated (Chang *et al.*, 2008). The L an R residues on the pentameric sequence R/QnLnE/Q/D, are important for processing and exit from the ER (Crabb *et al.*, 2010). The *Plasmodium* translocon of exported proteins (PTEX) traffics the proteins across the PVM and consists of five proteins (PTEX150, PTEX88, TRX2, Hsp101, EXP2). Of the five proteins, EXP2 forms a pore through which proteins are threaded after unfolding by HSP101 in an energy-dependent process (Matthews *et al*., 2013). Due to proteins being maintained in unfolded and extended state for export, there is need for a robust protein folding machinery to facilitate protein homeostasis.

1.6. Molecular chaperones

Molecular chaperones are proteins which interact with non-native states of other proteins but are not part of the final folded structures (Bukau *et al*, 2006). Molecular chaperones oversee the folding of newly synthesized polypeptides and the assembly of multisubunit structures (Saibil, 2013). In addition, molecular chaperones also maintain the unfolded states of proteins to facilitate their translocation across membranes (Kim *et al*., 2013). They also stabilize inactive forms of proteins which are turned on by cellular signals (Kim *et al*., 2013). During heat shock or cell stress there is an increase in cellular protein misfolding (Bukau *et al*., 2006). Some molecular chaperones are upregulated in response to stress, including heat are classified as heat shock proteins (Hsps) (Lindquist and Craig, 1988).

1.6.1. Heat shock proteins

Hsps are molecular chaperones that facilitate protein folding and protein disaggregation (Shonhai, 2008). The expression of Hsps responds to environmental changes experienced during the life cycle of the parasite (Edkins and Boshoff, 2014). Hsps are ubiquitous and

function to maintain protein homeostasis within the parasite during cell stress such as heat shock (Bukau *et al*, 2006). These proteins are highly conserved, occurring in most living organisms (Li and Srivastava, 2004). Hsps are classified into families based on their average molecular weight size in kDa. They belong to classes such as, Hsp110 (110 kDa), Hsp70 (70 kDa) and Hsp40 (40 kDa) (Table 1.1; Joly *et al*., 2010).

Table 1.1. Heat shock protein families and their general functions

Hsp	Average Molecular size (kDa)	Location in eukaryotes	Functions
Hsp 40	40	cytosol, mitochondria, nucleus	stabilization of misfolded proteins, co-chaperone for Hsp70[a]
Hsp 60	60	mitochondria	participates in protein folding and re-folding[b]
Hsp70	70	cytosol, mitochondria, nucleus	protein folding, membrane transport of proteins[c]
Hsp 90	90	cytosol, nucleus	regulatory interaction with signalling proteins, stabilization of misfolded proteins, prevents the aggregation of other proteins[d]
Hsp 100	100	cytosol, nucleus	protein dissaggregation, thermotolerance[e]
Hsp110	100-150	cytoplasm, endoplasmic reticulum (ER)	NEF[f], thermo tolerance[g]

Table legend: Hsp- heat shock protein, NEF- nucleotide exchange factor. (a) Botha *et al*., 2007; (b) Shonhai *et al*., 2007; (c) Bukau and Walker., 1990; (d) Yang *et al*., 2015; (e) Shonhai *et al*., 2005; (f) Zininga, 2015; (g) Dragovic *et al*., 2006.

1.6.2. Heat shock protein 40

Hsp40 family members are categorized into type I, II, III and IV based on the structure and function (Botha *et al*., 2011). The distribution of Hsp40s varies in different organisms, at least 51 are found in *P. falciparum* and approximately 50 are found in humans (Qiu *et al*., 2006; Kampinga *et al*., 2009; Njunge *et al*., 2013). The Hsp40s contain the highly conserved J-domain which possesses 70 amino acid residues (Li *et al*., 2009). A tripeptide histidine-proline-aspartic acid (HPD) motif forms part of the J-domain and functions in facilitating the formation of the Hsp40-Hsp70 complex (Hennesy *et al*., 2005; Bascos *et al*, 2017). The J-domain of types I and II Hsp40s is located at the N-terminus (Njunge *et al*., 2013). However, in types III and IV Hsp40 the J-domain could be located at any position within the protein (Njunge *et al*., 2013). Although Hsp40 type III and IV are similar, the J-domain of the type IV Hsp40 lacks the HPD motif (Kampinga and Craig, 2010). Both Hsp40s type I and II have a peptide-binding fragment located at the C-terminus of the proteins which is connected to the N-terminal J-domain via a G/F rich linker in both types (Kampinga and Craig, 2010). Type I Hsp40s contain unique Zinc-

finger motif between the J-domain and the C-terminal peptide-binding fragment (Kampinga and Craig, 2010).

Hsp40 serves as a co-chaperone of Hsp70 (Section 1.6.3) to promote protein folding, protein transport and degradation (Bukau and Horwich., 1998; Hennessy *et al*., 2005). The J-domain of Hsp40s binds to Hsp70 N-terminal ATPase domain. The binding regulates and stimulates the Hsp70 intrinsic ATPase activity (Wittung-Stafshede *et al.*, 2003). Hsp40 C-terminal peptide-binding fragment interacts with non-native polypeptides and suppresses protein aggregation (Li *et al.*, 2009). In *P. falciparum* Hsp40s are amongst the proteins exported to the erythrocyte cytosol, due to the presence of the *Plasmodium* export element (PEXEL) motif on some of them (Botha *et al.*, 2007; Njunge *et al.*, 2013). The motif targets the protein to the erythrocyte cytosol (Figure 1.2; Section 1.5).

1.6.3. Heat shock protein 70

Hsp70 is a group of proteins which are localized in different cellular compartments such as in the ER lumen, mitochondrial matrix and the cytosol of eukaryotic cells (Botha *et al*., 2007). Hsp70 is also involved in assembly of newly synthesized proteins (Multhoff *et al*., 2015), refolding of misfolded proteins (Szabo *et al*., 1994), disaggregation of proteins (Mayer, 2013), membrane translocation of organelle and secretory proteins (Hartl, 1996; Mayer and Bukau, 2005), and control of the activity of regulatory proteins (Radons, 2016). Hsp70s have an average molecular weight of 75 kDa (Kampinga *et al*., 2009). Hsp70s structurally consist of two major domains: N-terminal ATPase domain of 45 kDa (NBD) and the C-terminal substrate binding domain (SBD) of 25 kDa (Swain *et al*., 2007; Figure 1.3). The Hsp70-SBD is further sub-divided into a β-domain, containing the substrate binding pocket, and a α-helical lid (Wang *et al*., 1993). The SBD and the ATPase domain are joined by a flexible linker region, considered to facilitate inter-domain communication (Sharma and Masison, 2009).

Figure 1.3. The schematic representation of Hsp70
The diagram of Hsp70 showing the NBD-nucleotide binding domain, SBD-substrate binding domain, NH_2 terminal and CH terminal (Zininga, 2015).

1.6.4. Heat shock protein 110

Hsp110s are proteins that are overexpressed in response to cellular heat stress (Oh *et al.*, 1999). Hsp110s have been shown to have the ability to prevent protein aggregation and keep denatured protein in a folding-competent state (Dragovic *et al*., 2006). Hsp110s have similar NBD and SBD structure as their Hsp70 counterparts and bind misfolded protein substrates to act as holdases (Dragovic *et al*., 2006). Hsp110s hold client proteins in a folding competent manner under physiological stress (Goeckeler *et al*., 2002). Unlike the canonical members of Hsp70s, Hsp110s exhibit unique response to ATP-driven allostery (Raviol *et al*., 2006; Zininga *et al*., 2016). Hsp110s are known to be nucleotide exchange factors (NEF) for Hsp70s (Dragovic *et al*., 2006; Rampelt *et al*., 2018). NEFs catalyze the release of ADP from Hsp70, allowing the binding of ATP (Rampelt *et al*., 2018). Hsp110 homologues significantly enhance protein re-folding by canonical Hsp70 (Dragovic *et al*., 2006; Rampelt *et al*., 2018).

In *P. falciparum* the Hsp110 family members are PfHsp70-y and PfHsp70-z (Shonhai *et al*., 2007). PfHsp70-y has molecular mass of 108 kDa and is localized in the ER (Shonhai *et al*., 2007). PfHsp70-y contains a predicted apicoplast targeting signal containing an N-terminal leader sequence which is bipartite and comprises a signal peptide followed by a transit peptide. In addition, PfHsp70-y contains a C-terminal ER retrieval sequence which is suggested to be dominant. PfHsp70-y could function as a NEF for PfHsp70-2 (Shonhai *et al*., 2007).

PfHsp70-z has a molecular weight of 100 kDa (Table 1.2) and is a thermostable molecular chaperone that is suggested to act as a NEF for PfHsp70-1 (Zininga *et al*., 2016). PfHsp70-z shows low conservation in the substrate binding domain but has a relatively conserved ATPase domain (Shonhai *et al*., 2007; Zininga *et al*., 2016). In contrast to Hsp70 proteins, Hsp110 members possess an extended lid segment (Oh *et al*., 1999). The proteome of the malaria parasite is rich in proteins containing asparagine repeats making them prone to aggregation under heat stress (Singh *et al*., 2004; Pallarès *et al*., 2018). PfHsp70-z is believed to be able to suppress the aggregation of asparagine repeat-rich proteins more efficiently than its eukaryotic orthologs (Muralidharan *et al*., 2012). PfHsp70-z is considered to be a potential drug target and has been shown to be inhibited by both polymyxin B (PMB) (Zininga *et al*., 2017a) and (−)-Epigallocatechin-3-gallate (EGCG) (Zininga *et al*., 2017b).

1.6.5. Hsp70 functional cycle

Hsp70 collaborates with its co-chaperones to interact with synthesized proteins to ensure that the correct native conformation is achieved (Saibil, 2013). Hsp70 binds hydrophobic patches

of polypeptides via its SBD, including newly synthesized linear poly-peptides and partially folded proteins (Evans *et al.*, 2010). Hsp40 is required for substrate recruitment, it binds unfolded or misfolded protein and delivers them to the ATP-bound Hsp70 (Evans *et al.*, 2010). Hsp40 also stimulates ATP hydrolysis which increases the substrate affinity of the SBD (Kityk *et al.*, 2012). This results in Hsp70 conformational change to an ADP bound Hsp70 state and the C-domain covers the bound substrate providing a lid (Evans *et al.*, 2010; Kityk *et al.*, 2012). This is followed by subsequent binding of a NEF to the ADP-bound Hsp70 to facilitate the exchange of ATP resulting in the indirect release of the refolded substrate (Kityk *et al.*, 2012).

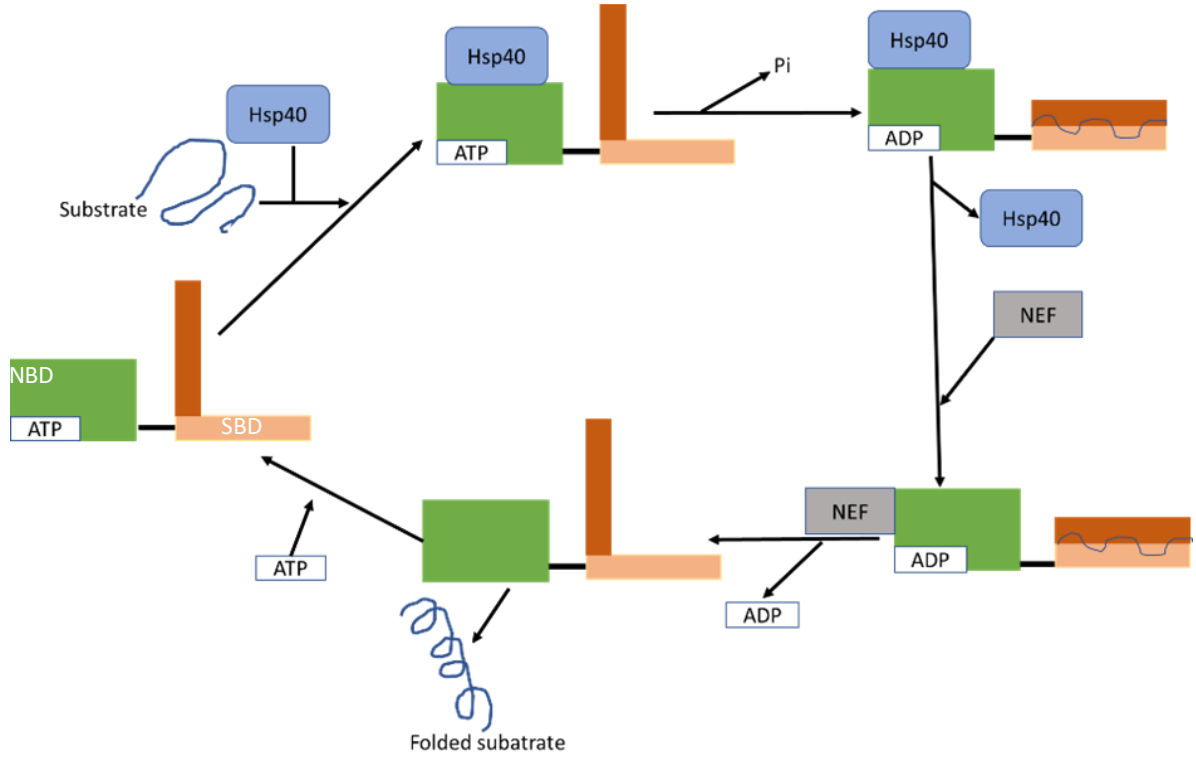

Figure 1.4. The functional cycle of Hsp70
The ATP-dependent reaction cycle of Hsp70, which is regulated by the J-domain proteins and nucleotide-exchange factors (NEFs) adapted from Evans *et al* (2010).

1.6.6. *Plasmodium falciparum* Hsp70

P. falciparum encodes for six Hsp70 (PfHsp70) proteins localized within different cellular compartments of the parasite (Table 1.2; Shonhai, 2010). Only PfHsp70-x is exported to the cytosol of the infected erythrocyte throughout different stages of the parasite's development (Külzer *et al.*, 2012).

Table 1.2. *P. falciparum* Hsp70 proteins and their functions

Class	Mass (kDa)	Localization	Functions
PfHsp70-1 (PF3D7_0818900)	74	nucleus, cytoplasm	protein folding[a] suppresses protein aggregation[b]
PfHsp70-2 (PF3D7_0917900)	73	ER	import of *P. falciparum* protein into ER protein folding and quality control in the ER[a]
PfHsp70-3 (PF3D7_1134000)	73	mitochondria	import of proteins into the mitochondrial matrix[a]
PfHsp70-x (PF3D7_0831700)	76	erythrocyte cytosol	exported to the infected erythrocyte[c]
PfHsp70-y (PF3D7_1344200)	108	ER	NEF for PfHsp70-2[d]
PfHsp70-z (PF3D7_0708800)	100	cytosol	NEF of PfHsp70-1 prevents aggregation of *P. falciparum* Asn repeat containing proteins[e]

Table legend: Asn- asparagine, NEF- nucleotide exchange factor, BiP-Binding immunoglobulin protein, ER-endoplasmic reticulum. References: (a) Shonhai *et al.*, 2007; (b) Przyborski *et al.*, 2015; (c) Kulzer *et al.*, 2012; (d) Shonhai, 2014; (e) Muralidharan *et al.*, 2012.

1.6.7. Cytosol localized Hsp70 of *Plasmodium falciparum*

PfHsp70-1

PfHsp70-1 facilitates protein quality control and is expressed throughout the erythrocytic stages of the parasite life cycle (Pesce *et al.*, 2008; Shonhai, 2014). PfHsp70-1 is a thermostable chaperone that facilitates folding of proteins and is robust at suppressing protein aggregation (Shonhai *et al.*, 2008; Misra and Ramachandran, 2009). PfHsp70-1 is also implicated in the transfer of misfolded proteins for degradation by the proteasome (Misra and Ramachandran, 2009; Przyborski *et al.*, 2015). In addition, PfHsp70-1 is involved in cyto-protection of the parasite during its life cycle within the host (Pesce *et al.*, 2008; Shonhai *et al.*, 2011)

1.6.8. Hsp70 resident in the endoplasmic reticulum of *Plasmodium falciparum*

PfHsp70-2

PfHsp70-2 is localized in the ER, it possesses the ER N-terminal leader sequence and a possible C-terminal ER retention signal KDEL (Shonhai *et al.*, 2007). Interestingly, the PfHsp70-2 homolog GRP78 is translocated to the cell surface under non-stressed conditions (Tsai and Lee, 2018). PfHsp70-2 has been implicated in protein secretion and degradation processes associated with the ER (Tuteja, 2007; Przyborski *et al.*, 2015). PfHsp70-2 has chaperone activity and has been proposed to be involved in the secretory pathway, working closely with the translocon machinery (Figure 1.4; Tuteja, 2007; Spork *et al.*, 2009). In addition, PfHsp70-

2 facilitates the import of proteins into the ER and to ensure they are folded properly (Shonhai, 2007; Przyborski *et al.*, 2015).

1.6.9. Mitochondrial *Plasmodium falciparum* Hsp70

PfHsp70-3

PfHsp70-3 is localized in the mitochondrion (Shonhai, 2007). Protein import to the mitochondrion is a post-translational event, and thus proteins must be kept in an unfolded state during their translocation (Figure 1.5; Przyborski *et al.*, 2015). PfHsp70-3 is suggested to function in protein import in the mitochondria with the aid of the PfHsp70-1 protein on the cytosolic side (Przyborski *et al.*, 2015). Since PfHsp70-3 is prone to aggregation it requires Hsp70 escort protein (Hep) to facilitate folding into active conformation and inhibit self-aggregation (Boshoff *et al.*, 2018). The PfHsp70-1 maintains the proteins in extended form for transport across the translocase of the outer membrane complex (Tom) (Njunge *et al.*, 2013). PfHsp70-3 is thought to pull the peptide through the inter-membrane space into the translocase of the inner membrane (Tim23) complex (Pfanner and Wiedemann, 2002; Boshoff *et al.*, 2018). It is suggested that PfHsp70-3 may also play a role in transport of proteins to the apicoplast, a secondary endosymbiotic organelle which is related to chloroplasts (Misra and Ramachandran, 2009).

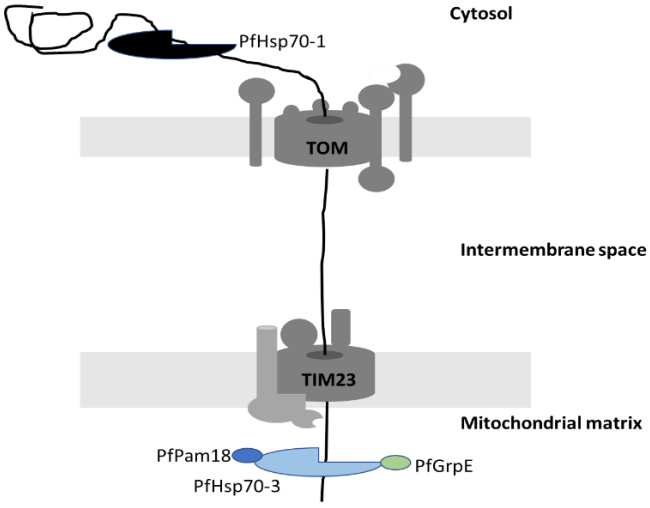

Figure 1.5. The role of PfHsp70-3 in the import of proteins into the mitochondrial matrix
Preproteins bound by PfHsp70-1 and extended to allow the peptide to thread TOM complex. The PfHsp70-3 and PfPam18 proteins assist the preproteins through the intermembrane space and thread through the Tim complex. The activity of PfHsp70-3 is modulated by GrpE and Hsp40s resident in the mitochondria. Adapted from Zininga, (2015).

1.6.10. Erythrocyte exported Hsp70

PfHsp70-x is exported to the erythrocyte cytosol and to the parasitophorous vacuole (PV) (Table 2; Külzer *et al*., 2012). Once the protein has been exported to the RBCs cytosol, it is co-localized with *P. falciparum* Hsp40 in small punctate structures known as "J-dots" (Külzer *et al*., 2012). Hsp70-x is unique to *P. falciparum* and the chimpanzee parasite *P. reichenowi* (Przyborski, 2015). The protein is closely associated with the *P. falciparum* erythrocyte membrane protein 1 (PfEMP1) (Charnaud *et al*., 2017). PfHsp70-x is implicated in protein trafficking across the PV possibly as an associated factor of the *Plasmodium* translocon of exported proteins (PTEX) (Charnaud *et al*.,2017).

PfHsp70-x is exported to the host cell throughout the different developmental stages of the parasite at the erythrocytic stages (Külzer *et al*., 2010). PfHsp70-x does not possess the PEXEL/HT signal which is involved in parasite export (Hiller *et al*., 2004; Marti *et al*., 2004). It is believed that secretion of the protein to the PV is facilitated by the first 25 amino acids, the so-called ER signal sequence (Figure 1.6; Külzer *et al*. 2012).

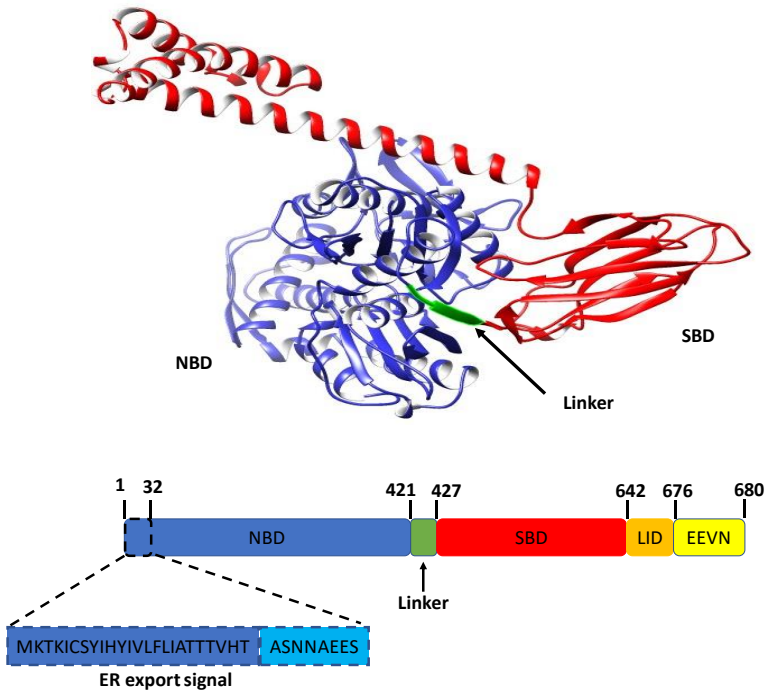

Figure 1.6. 3D model and schematic diagram of PfHsp70-x
PfHsp70-x is structurally composed of nucleotide binding domain (NBD)(Blue), substrate binding domain (SBD) (Red) which are joined by a linker (Green). The ER export signal at the NH_2 terminal and the CH terminal EEVN motif (yellow) are also represented in the schematic diagram (Rhiel *et al*., 2016). The 3D model was generated by Phyre2 (www.sbg.bio.ic.ac.uk/phyre2) and visualized using Chimera (www.cgl.ucsf.edu/chimera; Pettersen *et al*., 2004).

The eight amino acid sequence (**ASNNAEES**) located in the N terminal region of PfHsp70-x from amino acid position 25 to 32 acts as an ER export signal. This signal is responsible for the trafficking of the protein to the erythrocyte cytosol (Kulzer *et al*., 2012).

1.7. Innate immune response to malaria

Innate immune response is important in the control of primary *Plasmodial* malarial infection. Immune response against *P. falciparum* comprises of a cell mediated response which resulted from thousands of years of co-evolution between the parasite and its host (Artavanis-Tsakonas and Riley, 2002). Natural killer (NK) cells are important effectors of the innate immune response and amongst the first cells in peripheral blood to produce interferon gamma (IFN-γ) in response to the presence of *P. falciparum*-infected erythrocytes (Chen *et al*., 2014). Resistance to malaria is linked to early production of IFN-γ, interleukin (IL)-12, IL18 and tumor necrosis factor (TNF)-α. Additionally IFN-γ response in humans is associated with lower susceptibility to infection (Artavanis-Tsakonas and Riley, 2002; Menard and Dondorp, 2017).

Dendritic cells (DCs), macrophages, T cells and NK cells recognize parasite ligands such as ring-infected erythrocyte surface antigen (RESA), hypoxanthine guanine xanthine phosphoribosyl transferase (HGXPRT) and merozoite surface protein 1 (Roetynck *et al.*, 2006). DCs respond to parasite antigens recognized by pattern-recognition receptors (PRRs), such as Toll-like receptors (TLRs) and CD36 (Chen *et al*., 2014). NK cells induce production of IFN-γ resulting in DC maturation and their migration to the spleen (Roetynck *et al.*, 2006). The maturation of DCs is associated with the upregulation of MHC class II molecules, adhesion molecules and the production of cytokines (such as IL-12) (Dalod *et al*., 2014). The IL-12 cytokine activates NK cells inducing their cytolytic activity (Roetynck *et al.*, 2006). IL-2 produced by antigen-specific TH1 cells further activates NK cells to produce IFN-γ (Roetynck *et al.*, 2006). NK cells monitor the level of class I MHC molecules through activation and inhibitory NK cell receptors (Mavoungou, 2006). Class I MHC down-regulation by transformation or infection results in reduced inhibition of NK cells making the infected cells susceptible to NK cell lysis (Ida *et al*., 2005). Reduced levels of class I MHC molecules triggers release of granzyme B from intracellular granules resulting in the apoptosis of infected cells (Ida *et al*., 2005; Table 1.3).

1.7.1. Human granzymes

NK cells small cytoplasmic granules contain proteins such as perforin and proteases known as granzymes (Mavoungou, 2006). There are five granzymes in humans exhibiting unique substrate specificities and cleavage sites (Bratke *et al*., 2005; Table 1.3).

Table 1.3. Human granzyme B isoforms

Protein	Mode of action	Cleavage site
Granzyme A (GrA)	targets nuclear proteins for degradation such as histones, the lamins and DNA damage repair proteins (Ku70, PARP-1)[a]	basic residues[a]
Granzyme B (GrB)	activates caspase-3 (C-3) which in turn cleaves the N-peptide of procaspase-7 (C-7), making it accessible to maturation. The executioner C-7 then causes proteolysis of key cytosolic and nuclear substrates[b].	adjacent to acidic residues, particularly Asp[b]
Granzyme K (GrK)	function independently of caspase activation hydrolyzes the nucleosome assembly protein SET. Cleavage of SET by GrK inhibits its nucleosome assembly activity[c].	basic residues[c]
Granzyme H (GrH)	Unknown	Phe or Tyr at the P1 position[d]
Granzyme M (GrM)	mechanism of action not fully understood efficiently induce cell death in tumor cells and inhibit cytomegalovirus replication in a noncytotoxic manner[d].	residues with long, uncharged side chains (Met, Leu)[e]

Table legend; PARP1- poly [ADP-ribose] polymerase 1. References: (a) Zhu *et al*., 2006, (b) Metkar *et al*., 2003, (c) Zhao *et al*., 2007, (d) Sedelies *et al*., 2004, (e) de Poot and Bovenschen, 2014.

1.7.1.1. Granzyme B

Granzyme B (GrB) is a serine protease with a molecular weight of 32 kDa found in lytic granules of natural killer (NK) cells and cytotoxic T lymphocytes (CTL) (Rousalova and Krepela, 2010; Turner *et al*., 2017). The GrB shares Asp-ase (cleaving after aspartic acid) specificity with the large family of cell death cysteine proteases called caspases (Eliseo *et al*., 2016). GrB triggers an endogenous cell death cascade by activating target cell caspases (Metkar *et al*., 2003; Figure 1.7).

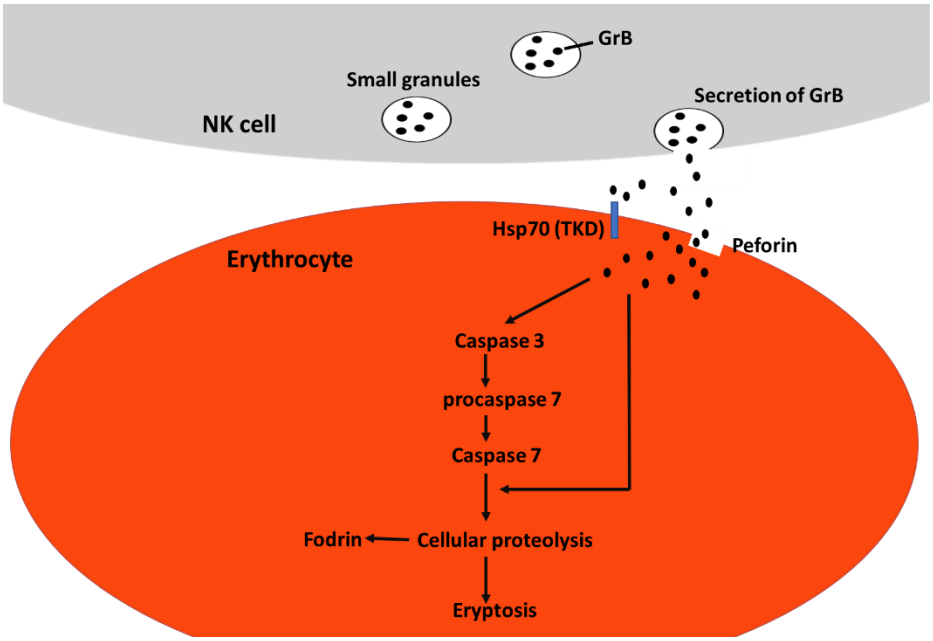

Figure 1.7. Hypothetical interaction between GrB with the TKD motif resulting in eryptosis
Natural killer cells utilize the exocytosis of cytotoxic granules containing perforin and granzymes (including granzyme B, GrB) from the NK cell. Once exocytosed, perforin homopolymerises in the membrane in a calcium-dependent manner and enables the release of GrB into the target cell cytosol. The activation of caspase-3 (C-3) by GrB results in the cleavage of the N-peptide of procaspase-7 (C-7), resulting in maturation. The executioner C-7 then causes proteolysis of key cytosolic and nuclear substrates.

1.8. Research motivation

There has been some success in the effort to reduce the malaria burden, and deaths from 607 000 in 2010 to 435 000 in 2017 (WHO, 2018). Despite these successes malaria continues to be a burden, mostly affecting children who account for two thirds of global malaria deaths (WHO, 2018). This is due to malaria affecting children who have not yet developed protective immune mechanisms. The persistence of malaria is mostly due to the emerging drug resistant parasite strains which reduces the effectiveness of antimalarial drugs (Cui *et al*., 2015). Parasite resistance to ACTs (Section 1.3) which have replaced mono-therapy as first line treatment has been reported. There are no current antimicrobial drugs to replace ACT (WHO, 2016). Therefore, there is a high need for new antimalarial drugs.

Some heat shock proteins are considered to be essential to parasites survival within the host making these proteins ideal drug targets (Zininga and Shonhai, 2014). In tumour cells, cell surface bound Hsp70s increased sensitivity to the cytolytic attack mediated by NK cells (Gross *et al*., 2003). Cell surface bound Hsp70 possess the extracellular localized recognition site for NK cells which is a 14 amino acid sequence TKD (TKDNNLLGRFELSG, amino acid 450–463) motif (Gross *et al*., 2003; Böttger *et al*., 2012). The Hsp70 TKD motif is thought to interact with human GrB resulting in cell death (Gross *et al*., 2003; Multhoff., 2007). PfHsp70-x also

possesses a TKD motif and thus may possibly interact with GrB. It is important to consider that the erythrocyte also has a resident human Hsp70 which may also interact with GrB but due to the erythrocyte's lack of a nucleus only the parasite PfHsp70-x can be upregulated in response to stress. This study sought to investigate the possible interaction between PfHsp70-x with GrB. In addition, this study sought to evaluate the anti-plasmodial properties of GrB.

1.9. Hypothesis

Surface exposed PfHsp70-x interacts with human GrB resulting in eryptosis.

1.10. Objectives and aims

1.11. Main aim

To investigate the possible direct protein-protein interaction of PfHsp70-x with GrB

1.12. Specific objectives

1. Biophysical characterization of PfHsp70-x and hHsp70

Approach: The comparison of the secondary and tertiary structures of the proteins was conducted using Circular dichroism (CD) spectroscopy and Tryptophan fluorescence.

2. Investigation of the direct protein-protein interaction of PfHsp70-x and hHsp70 with human Granzyme B

Approach: The comparative capabilities of PfHsp70-x and hHsp70 to interact with human Granzyme B were evaluated using slot blot and ELISA

3. To determine the toxicity of Granzyme B on *P. falciparum* 3D7-infected erythrocytes

Approach: Parasite growth inhibition assay was used to evaluate the anti-plasmodial effect of Granzyme B

2. Methods and materials

2.1. Materials

The plasmid constructs used were previously described (Table 2.1; Mabate *et al*., 2018). The DNA inserts were cloned into pQE30 plasmid between *Bam*HI and *Hind*III restriction sites. The pQE30/PfHsp70-xF (PF3D7_0831700) plasmid was used to express the full length PfHsp70-x, the pQE30/PfHsp70-xT plasmid construct was used to express the truncated PfHsp70-x which lack the EEVN motif. The pQE30/hHsp70 plasmid was similarly used towards expressing the human Hsp70 recombinant protein in bacteria (Monyai, 2018). The pQE30/PfHsp70-xF and pQE30/PfHsp70-xT constructs were used as previously described (Mabate *et al*., 2018). Reagents used are listed in (Appendix C: Table C1).

Table 2.1 *E. coli* strains and plasmid constructs used for expression of recombinant proteins

Competent cells	Description	Supplier/Reference
E. coli XL1 Blue	*rec*A1 *end*A1 *gyr*A96 *thi*1 *hsd*R17 supE44 *rel*A1*lac* (F´proAB *lac*IqZM15 Tn10 (Tetr)	Bullock *et al*., (1987)
E. coli BL21 Star (DE3)	*F- ompT gal [dcm] [lon] hsd*SB *λDEs*	Studier *et al*., 1990
E. coli JM109	*e14– (McrA–) recA1 endA1 gyrA96 thi-1 hsdR17 (rK – mK+) A1 Δ(lac-proAB) (F′ traD36 proAB lacIqZΔM15).*	Thermofisher Scientific, USA
Plasmid constructs	Description	Reference
pQE30/*PfHsp70-x*	pQE30 encoding PfHsp70-x, AmpR	Mabate *et al*., 2018
pQE30/*PfHsp70-xT*	pQE30 encoding PfHsp70-xT, AmpR	Mabate *et al*., 2018
pQE30/*hHsp70*	pQE30 encoding human Hsp70, AmpR	Monyai, 2018

2.2. Confirmation of plasmid constructs

Endonuclease restriction digest was conducted using *Bam*HI and *Hind*III fast digest restriction enzymes (Thermo scientific, USA) as their restriction sites flank the inserts. Samples were prepared and incubated at 37 °C for 15 minutes. A 0.8 % agarose gel was prepared in 1 M TAE (400 mM Tris, 0.1 % glacial acetic acid, 10 mM EDTA) and was used to analyze the digested products. The gel was visualized using ChemiDoc Imaging system (Bio-Rad, USA).

2.3. Expression of recombinant proteins

The plasmids, pQE30/PfHsp70-xF, pQE30/PfHsp70-xT and pQE30/hHsp70 were transformed into BL21 cells. The recombinant proteins were overexpressed in terrific broth (TB) (1.2 % tryptone, 2.4 % yeast, 0.5 % glycerol, 17 mM KH_2PO_4, 72 mM K_2HPO_4). The colonies were picked and grown for 24 hours in 50 ml broth containing 100 µg/ml ampicillin at 37 °C, then subsequently diluted using 450 mL respectively. The cells were further incubated at 37 °C with shaking at 160 g using FMH 200 shaker (FMH Electronics, RSA) to OD_{600} = 0.6. the expressions were induced using 1 mM isopropyl-β-D-1-thiogalactopyranoside (IPTG). The samples were harvested and centrifuged at 15 000 g for 60 seconds. The pellets were then re-suspended in 10 ml lysis buffer (10 mM Tris, pH 7.5, 300 mM NaCl and 10 mM imidazole containing 1 mM EDTA, 1 mM phenylmethylsulfonyl fluoride (PMSF) and 1 mg/ml lysozyme).

2.4. Purification of the Hsp70 proteins

The purification of the PfHsp70-xF, PfHsp70-xT and hHsp70 proteins was conducted as previously described (Zininga *et al.*, 2015; Mabate *et al.*,2018). Briefly, whole *E. coli* lysates previously frozen at -80 ºC freezer were thawed on ice. Polyethyleneimine (PEI) 0.1 % (v/v) was added to the lysates to solubilize the proteins and precipitate nucleic acids which may be linked to the protein leaving the target protein in the supernatant. The lysates were centrifuged at 5000 *g* for 20 minutes at 4 °C. The supernatants were loaded onto HisPur™ Nickel-charged nitrilotriacetic acid (Ni-NTA) immobilized metal affinity chromatography (IMAC) (Thermo Scientific, USA). The PfHsp70-x supernatants were incubated at 4°C for 4 hours to allow His_6-PfHsp70-x in the soluble cell extract to bind to HisPur™ Ni-NTA. The supernatants were then allowed to run through the column and the flow through fractions were collected for analysis. The columns were washed with wash buffer 1 (100 mM Tris pH 7.5; 300 mM NaCl, 25 mM imidazole and 1 mM PMSF) followed by wash buffer 2 (100 mM Tris pH 7.5; 300 mM NaCl, 80 mM imidazole and 1 mM PMSF). The bound proteins were eluted with elution buffer 1 (100 mM Tris pH 7.5; 300 mM NaCl, 250 mM imidazole and 1 mM PMSF), followed by elution buffer 2 (100 mM Tris pH 7.5; 300 mM NaCl, 500 mM imidazole and 1 mM PMSF). The washes and elutions were collected and analysed with SDS-PAGE and protein presence was confirmed using Western blot analysis (Monyai, 2018).

2.5. Investigation of the secondary structure and stability of the Hsp70 proteins

The secondary structures of recombinant PfHsp70-xF, PfHsp70-x T and hHsp70 were analyzed using Far-UV circular dichroism (CD). A J-1500 CD spectrometer (JASCO Ltd, UK) was used to conduct CD spectrometry experiments as previously described (Zininga *et al*., 2015) with minor modifications. Briefly, recombinant proteins (0.5 µM) were suspended in PBS (137 mM NaCl, 27 mM KCl, 4.3 mM Na_2HPO_4 and 1.4 mM KH_2PO_4, at pH 7.4) and analyzed using a 0.1 cm path-length quartz cuvette (Hellma). Spectra were averaged for least 7 scans after baseline correction (subtraction of spectrum from buffer in which the proteins were excluded). Secondary structure predictions were conducted as previously described (Zininga, 2015). The spectra were deconvoluted to α-helix, β-sheet, β- turn and unordered regions, using the Dichroweb server (CDSSTR reference database), (http://dichroweb.cryst.bbk.ac.uk) (Sreerama *et al*., 2000; Whitmore and Wallace, 2008).

The effect of chemical denaturation on the proteins was investigated using urea following a previously described protocol (Zininga, 2015). The effects of urea on the stability of the proteins were monitored by assessing the molar residue ellipticity at 222 nm, with temperature set at 20 °C in the absence and presence of varying urea concentration (0 M to 8 M). The folded states of the proteins were determined as previously described (Zininga *et al*., 2017):

$((\theta)t - (\theta)h) / ((\theta)l - (\theta)h)$ Equation 1

Where $(\theta)t$ is the molar ellipticity at any given urea concentration, $(\theta)h$ at highest concentration, and $(\theta)l$ at lowest concentration, respectively.

2.6. Assessment of the tertiary structure of Hsp70s

The tertiary structural organization of the PfHsp70-xF, PfHsp70-xT and hHsp70 proteins was assessed using tryptophan fluorescence as previously described (Zininga *et al*., 2015). Tryptophan fluorescence involved monitoring the changes in tertiary structure of the proteins that were subjected to urea denaturation. The recombinant proteins (2 µM) were incubated in PBS for 20 minutes at 20°C in the presence of variable urea concentrations (0 M- 8 M). Fluorescence spectra were recorded between 300 nm and 400 nm after initial excitation at 295 nm using JASCO FP- 8200 spectrofluorometer (JASCO).

2.7. Analysis of chaperone activity of Hsp70s by suppressing malate dehydrogenase (MDH) aggregation

The chaperone function of PfHsp70-xF, PfHsp70-xT and hHsp70 was investigated by monitoring their ability to suppress heat-induced aggregation of model substrate MDH from the *porcine* heart (Sigma-Aldrich) as previously described (Zininga *et al*., 2016; Mabate *et al*., 2018). Briefly, the chaperone function of each protein in suppressing thermally induced aggregation of MDH was monitored spectrophotometrically. MDH (0.6 µM) was added to the pre-heated buffer (50 mM Tris, pH 7.4, 100 mM NaCl) at 51 °C. The temperature was maintained at 51 °C for 80 minutes and the absorbance was monitored at 340 nm in 5 minute intervals. This assay was performed using SpectraMax M3 spectrometer (Molecular Devices, U.S.A). BSA was used as a non-chaperone control in this assay. The data were analyzed using GraphPad Prism 6.05 software.

2.8. Investigation of interaction of Hsp70s with human GrB using Slot blot

Direct protein-protein interaction studies of PfHsp70-x/ hHsp70 with Granzyme B were conducted using slot blot following the protocol previously described (Zininga *et al*., 2016). Briefly, varying concentrations (5 µg, 10 µg and 20 µg) of recombinant PfHsp70-xF, PfHsp70-xT and hHsp70 were immobilized onto nitrocellulose membrane using the Bio-Dot ^{TM}SF apparatus. In addition, 20 µg of bovine serum albumin (BSA) and human GrB were immobilized as negative and positive controls for GrB antibody respectively. The membranes were then blocked with 5 % skimmed milk prepared in Tris buffer saline (TBS) (50 mM Tris, 150 mM NaCl) pH 7.5 for an hour at 25 ^{o}C, followed by washing with TBST (TBS, 1 % Tween 20) three times for 15 minutes. Subsequently, the immobilized proteins were overlaid with GrB (10 µg/ml) prepared in 5 % skimmed milk and incubated overnight at 4 ^{o}C. After washing steps, the membranes were incubated with the mouse raised monoclonal α-GrB primary antibody [1: 2000] (Sigma-Aldrich, USA) followed by incubating with α-mouse IgG secondary HRP-conjugated antibody [1: 4000] (Sigma-Aldrich, USA). The immunoblots were visualized using chemiluminescent substrate (ECL) (Thermo scientific, USA) as per manufacturer's instructions. The images were captured using ChemiDoc Imaging system. The densitometric analysis was conducted using the Image Lab^{TM} software (Bio-Rad, USA).

2.9. Investigation of direct interaction between Hsp70s and GrB using Enzyme linked immunosorbent assay (ELISA)

The ELISA assay was used to validate the results obtained from the slot blot. A previously described protocol by (Biesiadecki and Jin., 2011) was followed for conducting the ELISA. Briefly, recombinant proteins (5 µg) PfHsp70-x, PfHsp70-x T, hHsp70 and BSA were immobilized on to the uncoated 96 well microtiter by passive adsorption using 5 mM sodium bicarbonate ($NaHCO_3$) at pH 9.5. The immobilized proteins were incubated overnight at 4 °C. After incubation the plate was washed once rapidly to remove unbound protein with TBST (TBS and 0.1 % Tween 20) buffer A. The wells were then blocked with 150 µL of 5 % skimmed milk prepared in TBS and incubated at 25 °C for 1 hour. The wells were then washed using buffer A three times for 10 minutes. Serial dilutions of the analyte GrB (0 -1000 nM), were prepared in 5 % skimmed milk prepared in TBS (buffer B) and a 100 µL of each dilution was added into the wells and incubated for 2 hours at 25 °C. The wells were then washed three times before addition of 100 µL of monoclonal α-GrB primary antibody (1:2000) in buffer B to each well and incubated for 1 hour at 25 °C. The secondary HRP conjugated α- mouse antibody (1:2000) in buffer B was then added to the well at 100 µL/well and incubated for 1 hour at 25 °C. The excess unbound antibody was washed three times for 10 minutes using buffer A. The 3,3',5,5'-tetramethylbenzidine (TMB) (Bioo Scientific, USA) was added to the wells at 100 µL/well and incubated for 2 minutes to allow for the substrate reaction. The SpectraMax M3 microplate reader (Molecular Devices, USA) was used to monitor the color development over 5-minute intervals for 30 minutes at 370 nm. The resulting absorbances were plotted against time. Furthermore, in order to investigate the effects of nucleotides on the interaction the assay was repeated in the presence of 5 mM ATP/ADP.

Data analysis

To determine the absorbances for each serial dilution of GrB, the background readings from uncoated and BSA negative control wells (which were treated in a similar manner to the assay wells) were subtracted from all absorbance readings as baseline readings. Subsequently, from the absorbance readings obtained, readings corresponding to the highest concentrations of GrB were averaged and considered to be the maximum (100 %) binding for the protein. Each serial dilution concentration absorbance of GrB was processed in relation to the average maximum binding. GraphPad prism 6.05 (GraphPad Software, USA) was used to plot a titration curve

against log scale and the curve was fitted to determine the equilibrium binding constant (Kd). The Kd is defined as the concentration of GrB required to reach 50% maximal binding.

2.10. Investigation of the anti-plasmodial activity of human Granzyme B

P. falciparum 3D7 parasites were grown and maintained in continuous culture as previously described (Trager and Jensen, 1976; Zininga *et al*., 2015). Briefly, malaria *P. falciparum* parasites were maintained in RPMI 1640 medium containing 2 mM L-glutamine and 25 mM Hepes (Lonza). Supplemented with 5 % Albumax II, 20 mM glucose, 0.65 mM hypoxanthine, 60 µg/mL gentamycin and 2-4 % hematocrit of human erythrocytes. The parasites were cultured at 37 ºC under 5 % CO_2, 5 % O_2, 90 % N_2 in sealed T25 culture flasks. For screening of GrB anti-plasmodial, the parasites at 0.1 % parasitemia were transferred into 96 well plate and incubated for 48 hours at 37 ºC. After 48 hours the plates are removed from the incubator. Followed by the removal of 20 µl of culture from each well and mixed with 125 µl of a mixture of Malstat solution and Nitro blue tetrazolium salt (160 mg) and phenazineethosulphate (8 mg) dissolved in H_2O (100 ml) (NBT/PES solution) in a fresh 96-well plate.

The *P. falciparum* lactate dehydrogenase (pLDH) method was used to monitor the growth of *P. falciparum* 3D7-infected erythrocytes subjected to different amounts of (0 –25 µg/mL) GrB treatments as previously described (Zininga *et al*., 2017). Initial growth assay screening was conducted at 25 µg/mL GrB concentration. The protein was further analysed for IC50 determination by titrating (range 0.001–20 µg/mL) the GrB concentration. Analysis of the pLDH data for growth inhibition assay was carried out using GraphPad Prism 6. All experiments in this study were repeated in triplicate.

3. Results

3.1. Confirmation of pQE30/PfHsp70-xF and pQE30/PfHsp70-xT constructs

Plasmid maps representing the pQE30/PfHsp70-xF and pQE30/PfHsp70-xT constructs were constructed (Figure 3.1A and B) and the integrity of the plasmids was verified by restriction digest using restriction enzymes, *Bam*HI and *Hind*III (Figure 3.1 C).

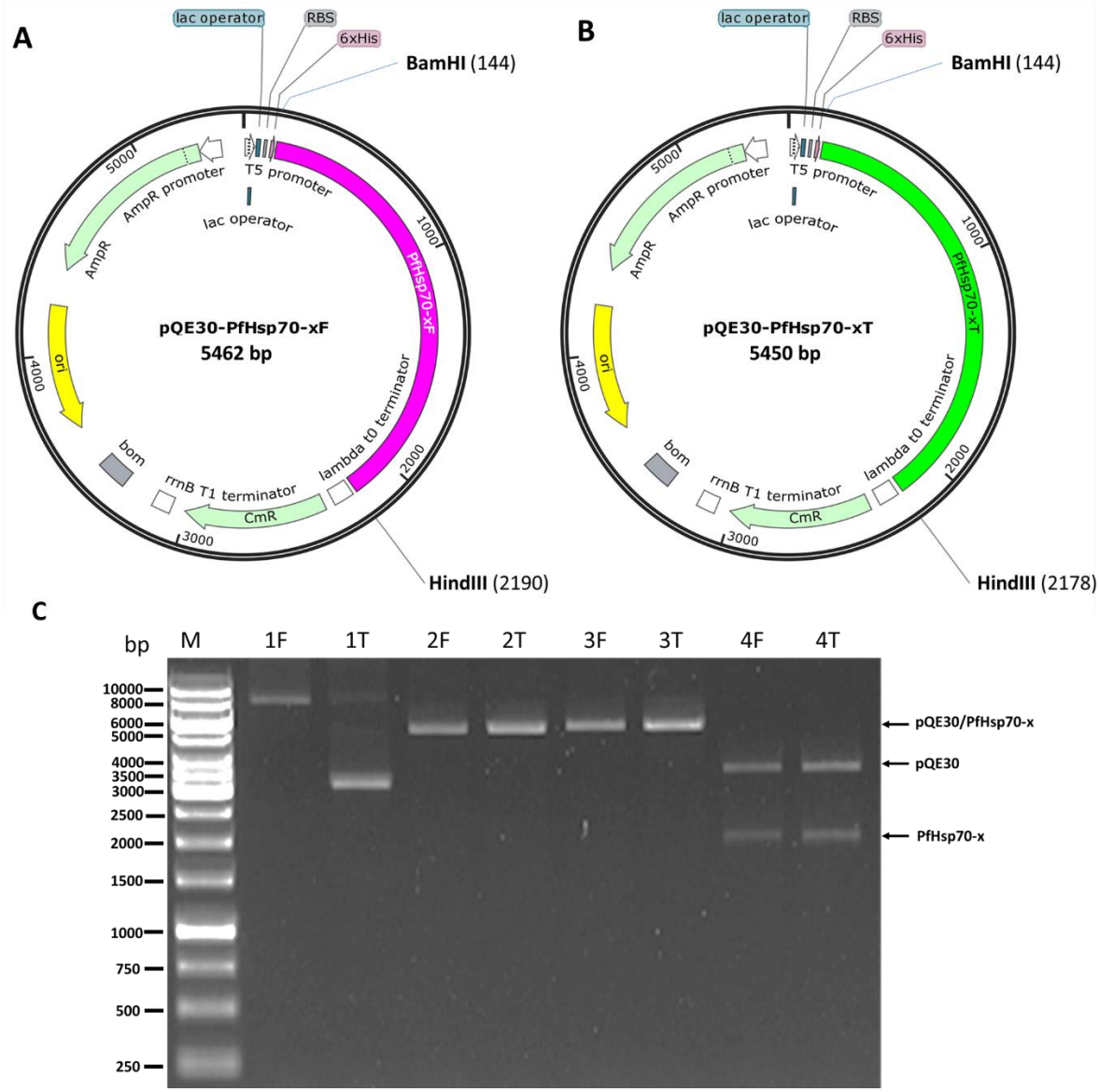

Figure 3.1. Verification of pQE30/PfHsp70-x and pQE30/PfHsp70-xT plasmid constructs
Restriction digest analysis of pQE30/PfHsp70-xF and pQE30/PfHsp70-xT. Plasmid maps of (A) PfHsp70-xF and (B) PfHsp70-xT showing the *Bam*H1 and *Hind*III restriction sites. (C) Agarose gel electrophoresis of pQE30/PfHsp70-xF and pQE30/PfHsp70-xT: lane M, DNA molecular weight maker in bp; The F and T next to the lane number indicate the pQE30/PfHsp70-xF and pQE30/PfHsp70-xT respectfully, lane 1, undigested pQE30/PfHsp70-xF and pQE30/PfHsp70-xT plasmids; lane 2, pQE30/PfHsp70-xF and pQE30/PfHsp70-xT digested with *Bam*HI; lane 3, pQE30/PfHsp70-xF and pQE30/PfHsp70-xT digested with *Hind*III; lane 4, pQE30/PfHsp70-xF and pQE30/PfHsp70-xT digested with both *Bam*HI and *Hind*III.

Single digestion of pQE30/PfHsp70-x and pQE30/PfHsp70-xT with either *Bam*HI or *Hind*III produced a linearized plasmid of sizes 5462 bp and 5450 bp respectively (Figure 3.1 C). Double digestion using both restriction enzymes resulted in a 3424 bp fragment in both constructs which corresponds to the pQE30 expression vector (Figure 3.1 C). In addition, the double digest of pQE30/PfHsp70-x and pQE30/PfHsp70-xT also resulted in a 2040 bp fragment for the PfHsp70-xF insert and a 2028 bp fragment for the PfHsp70-xT insert (Figure 3.1 C).

3.2. Confirmation of pQE30/hHsp70 construct

The integrity of pQE30/hHsp70 was verified by restriction digest *Bam*HI and *Hind*III (Figure 3.2). Single restriction digestion with either *Bam*HI or *Hind*III resulted in the migration of linearized plasmid of 5363 bp (Figure 3.2B). Double digestion using *Bam*HI and *Hind*III resulted in two fragments of 3424 bp and 1953 bp, corresponding to the pQE30 expression vector and hHsp70 insert sizes, respectively (Figure 3.2B).

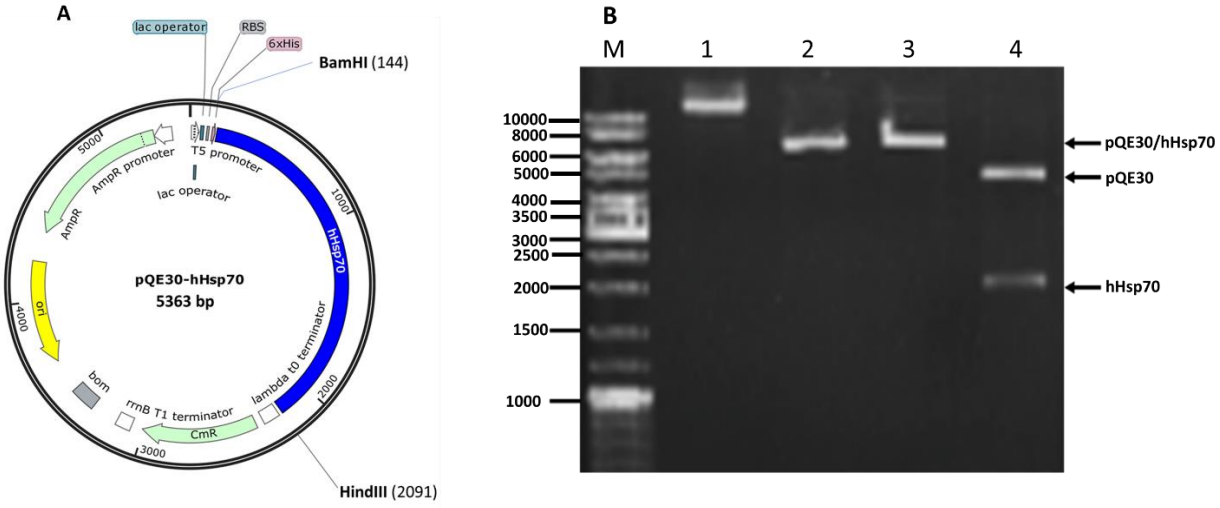

Figure 3.2. pQE30/hHsp70 plasmid restriction map and agarose gel confirmation
Restriction analysis of pQE30/hHsp70 DNA plasmid (A) Plasmid map of pQE30/hHsp70 showing the *Bam*HI and *Hind*III restriction sites. (B) Agarose gel electrophoresis of pQE30/hHsp70: lane M, DNA molecular weight (bp) maker; lane 1, undigested pQE30/hHsp70 plasmid; lane 2, pQE30/hHsp70 digested with *Bam*HI; lane 3, pQE30/hHsp70 digested with *Hind*III; lane 4, pQE30/ hHsp70 digested with both *Bam*HI and *Hind*III.

3.3. Expression and purification of recombinant PfHsp70-xF, PfHsp70-xT and hHsp70 proteins

The recombinant PfHsp70-xF and PfHsp70-xT proteins were successfully expressed in *E. coli* BL21 (DE3) cells (Figure 3.3). The production of PfHsp70-xF and PfHsp70-xT proteins, (Figure 3.3A and B respectively) was analyzed by SDS-PAGE and confirmed by Western blot analysis using α-PfHsp70-x. There was an increase in the level of expression of both PfHsp70-xF and PfHsp70-xT. The control which was *E. coli* BL21 (DE3) cells transformed with pQE30

vector confirmed the absence of recombinant Hsp70 in these cells as expected (Figure 3.3A and B). Western blot was used to confirm the presence of PfHsp70-x proteins. Although leaky expression of the protein species was observed (figure 3.3A and B), recombinant protein expression was successfully induced with IPTG (Figure 3.3A and B).

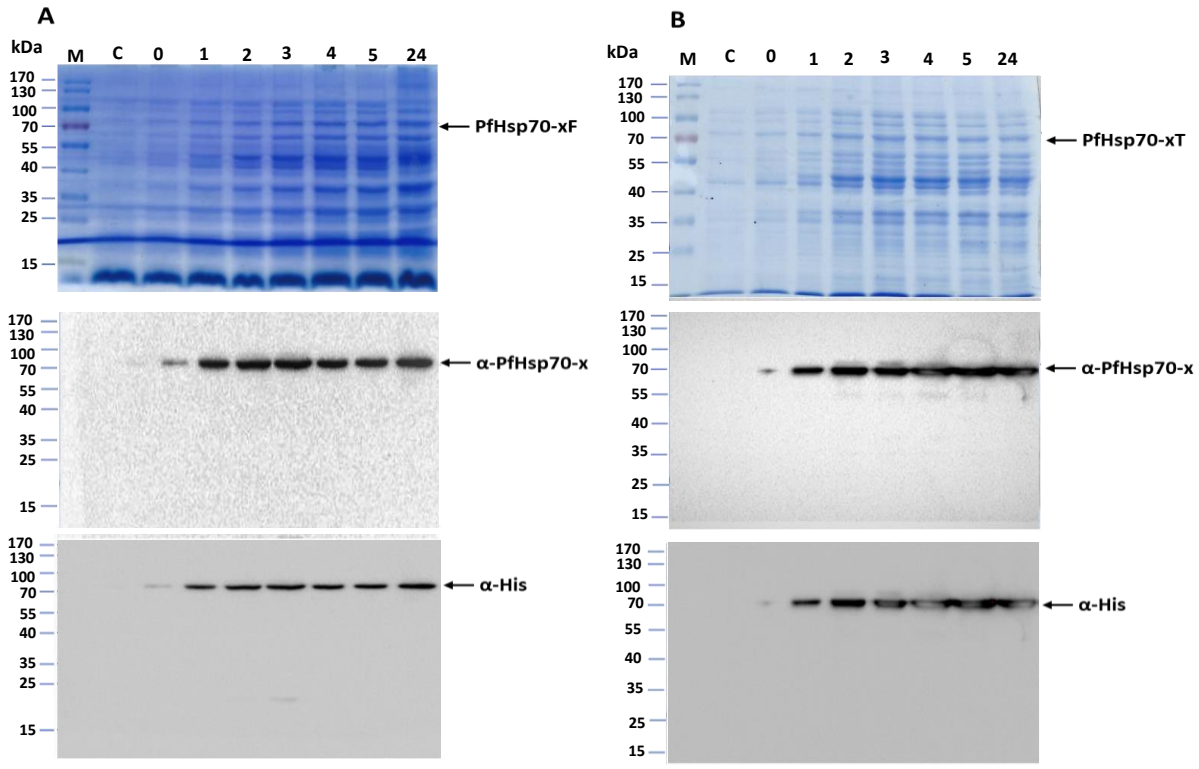

Figure 3.3. Expression of recombinant PfHsp70-x proteins
(A) PfHsp70-xF and (B) PfHsp70-xT were analyzed with SDS-PAGE and confirmed with Western Blot. Expression of recombinant PfHsp70-xF; lane M-Page ruler (Thermo Scientific, USA) in kDa; lane C-Total extract for cells transformed with pQE30 plasmid without insert; lane 0-total cell extract transformed with pQE30/PfHsp70-x(F/T) before IPTG induction; lanes 1, 2, 3, 4, 5 and 24 represent post induction samples collected at 1, 2, 3, 4, 5 and 24 hours respectively.

The expressed PfHsp70-xF and PfHsp70-xT proteins were successfully purified by affinity chromatography (Figure 3.4). PfHsp70-x proteins were loaded onto nickel beads and some of the protein was lost in the washes but eluted at approximately 76 kDa (Figure 3.4). Purifications of PfHsp70-xF resulted in a final protein yield of approximately 6 mg/l of protein and its truncated counterpart protein yield was 4 mg/l. The purification was confirmed using SDS-PAGE and Western blot conducted using α-PfHsp70-x antibodies and α-His antibodies respectively. Western blot confirmed that the PfHsp70-xF did not bind well to the beads as most of the protein was lost in the flow through and wash steps of the purification (Figure 3.4A).

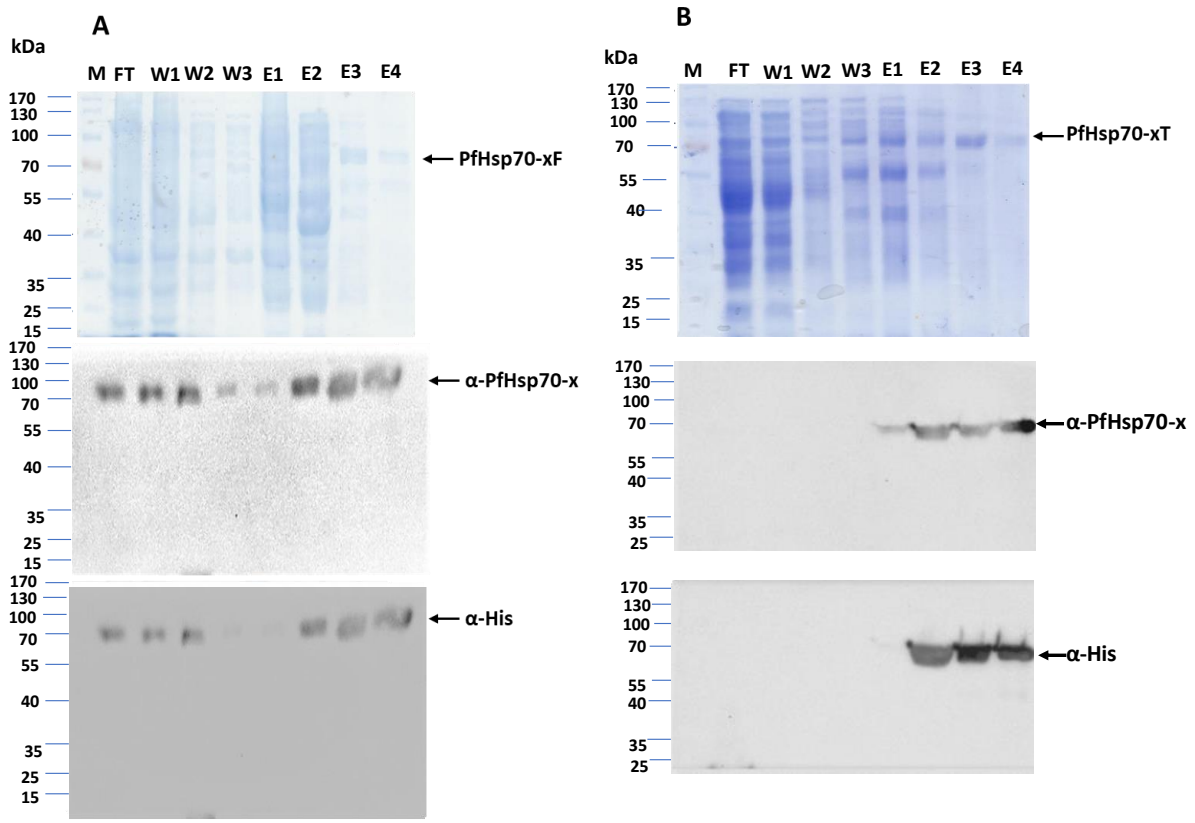

Figure 3.4. Purification of recombinant PfHsp70-x proteins
Purification of (A) PfHsp70-xF and (B) PfHsp70-xT was conducted using Nickel affinity chromatography; Lane FT-flow through; lane W-wash samples, and lane E-PfHsp70-xF/T protein eluted using 500 mM imidazole. Lower panels: Western blot based on use of α-PfHsp70-x and α-His antibodies purification of PfHsp70-x protein.

Recombinant hHsp70 protein was successfully expressed in BL21 (DE3) *E. coli* cells (Figure 3.5A). The production of the protein was analyzed by SDS-PAGE and confirmed by Western blot analysis using α-His (Figure 3.5A). The samples collected during expression showed an increase in the level of expression of a species at approximately 74 kDa size. The control which was *E. coli* BL21 (DE3) cells transformed with pQE30 vector confirmed the absence of 74 kDa species (Figure 3.5A). This suggests that the 74 kDa species expressed by the transformed cells was indeed recombinant hHsp70. Leaky expression of the protein species was observed (Figure 3.5A). However, expression was further induced by IPTG (Figure 3.5A).

The successful expression of recombinant hHsp70 was followed by purification using nickel affinity chromatography (Figure 3.5B). hHsp70 protein was loaded onto nickel beads and eluted at approximately 74 kDa (Figure 3.5B). The purification of hHsp70 resulted in a final protein yield of approximately 11 mg/L of protein. The product was analyzed with SDS-PAGE and confirmed with Western Blot using α-His antibodies.

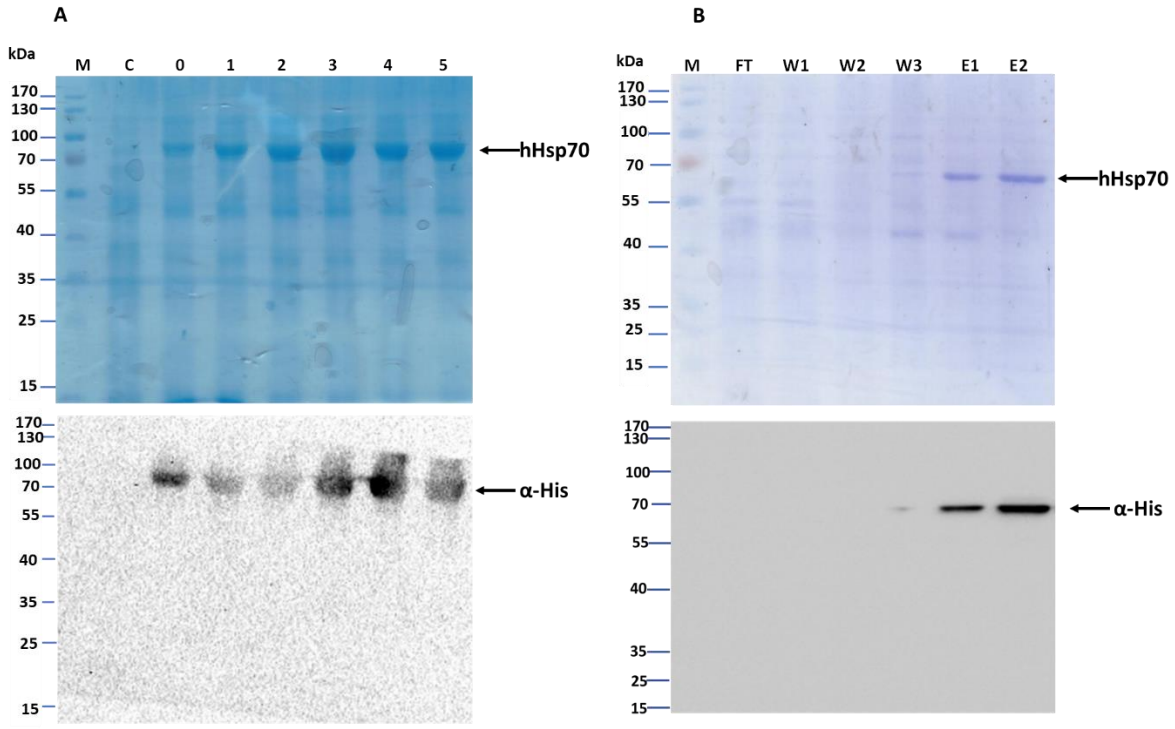

Figure 3.5. Expression and purification of recombinant hHsp70
The hHsp70 expression and purification was analyzed with SDS-PAGE and confirmed with Western Blot. (A) Expression of recombinant hHsp70; lane M-Page ruler (Thermo Scientific) in kDa; lane C-Total extract for cells transformed with pQE30 plasmid without insert; lane 0 –total cell extract transformed with pQE30/hHsp70 before IPTG induction; lanes 1, 2, 3, 4 and 5 post induction samples collected at 1, 2, 3, 4 and 5 hours respectively. (B) Purification of hHsp70 conducted using Nickel affinity chromatography; Lane FT- flow through; lane W-wash samples, and lane E-hHsp70 protein eluted using 500 mM imidazole.

3.4. Analysis of the secondary structure of Hsp70

To explore the secondary structures of PfHsp70-xF/PfHsp70-xT and hHsp70, CD spectrophotometric analysis was conducted. The recorded signals (experimental) between 190 nm and 240 nm were superposed to predicted signals obtained using Dichroweb (Figure 3.6A). The correlation between the two signals that were resolved using the CDSSTR method gave NRMSD values of approximately 0.002, representing a good correlation. For all three proteins the far UV spectra exhibited two negative depressions (troughs) at 209 and 221 nm, respectively (Figure 3.6A). This spectrum represents the helical character of the recombinant proteins.

In addition, the effect of urea on the secondary structure of PfHsp70-xF/PfHsp70-xT and hHsp70 was also investigated. The CD spectra measurements were repeated in the presence of varying concentrations of urea (Figure 3.6B), to determine if the protein structure is affected by urea. Secondary structure stability was subsequently monitored at 221 nm, as the proteins were exposed to increasing urea concentrations (Figure 3.6B). The urea based data served as

positive control, demonstrating that the proteins were folded as they responded to treatment by urea as a denaturant.

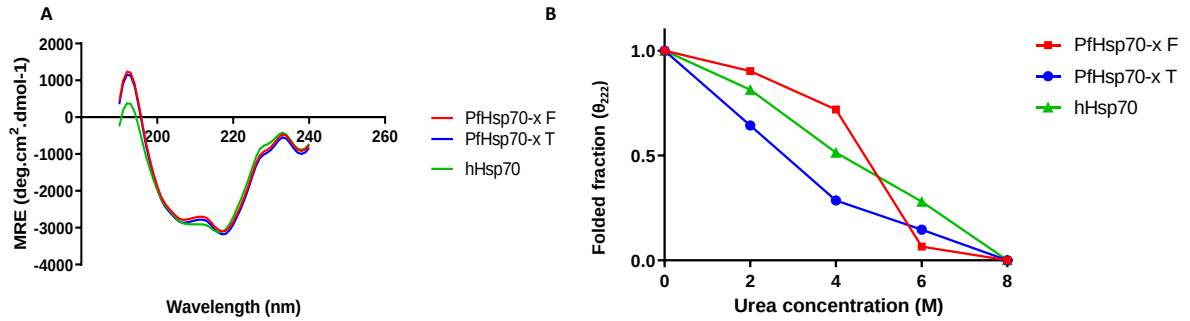

Figure 3.6. Secondary structure analyses using CD spectroscopy
(A) PfHsp70-xF, PfHsp70-xT and hHsp70 proteins far UV spectra showing two negative depressions (trough) at 209 and 221 nM, respectively. (B) Analysis of the effect of urea on the folded fraction of the proteins was conducted.

3.5. The tertiary structural organization of the Hsp70s

The tertiary structures of PfHsp70-xF, PfHsp70-xT and hHsp70 were evaluated using tryptophan-based fluorescence (Figure 3.7A). In addition, analysis of the proteins in the presence of variable levels of urea was conducted (Figure 3.7). The recombinant proteins tertiary structures were assessed in response to increasing urea concentration. The increase in urea concentration resulted in reduced tryptophan fluorescence signal, suggesting quenching of the relative fluorescence dependent on urea concentration (Figure 3.7B, C and D). PfHsp70-xF and PfHsp70-xT exhibited tryptophan fluoresce changes which registered a red shift, however the hHsp70 showed a blue shift (Figure 3.7E). The red shift indicates that the proteins acquired a more open conformation as the urea concentration increases. However, blue shift indicates that the hHsp70 acquired a closed conformation in response to presence of increased urea concentration.

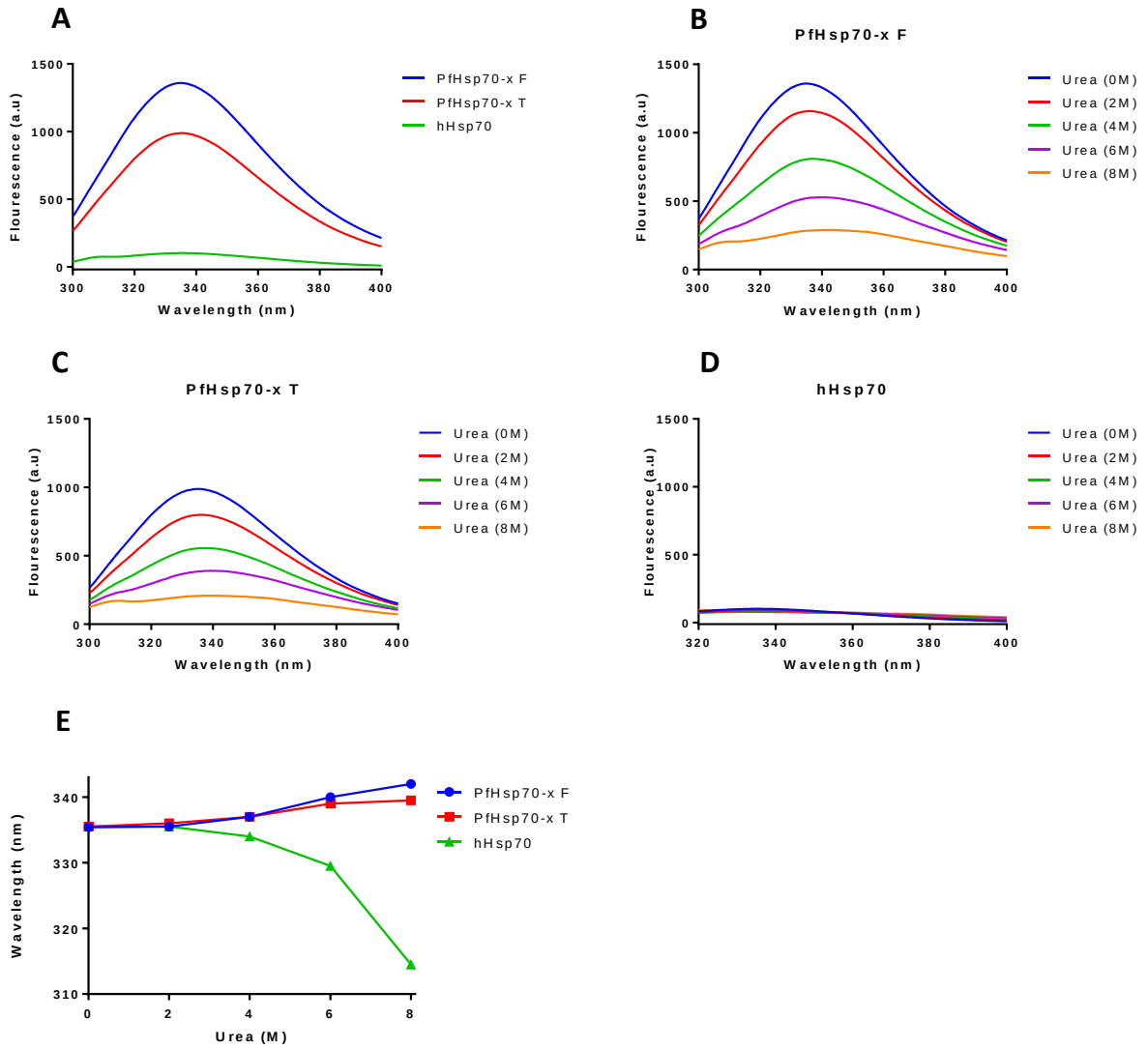

Figure 3.7. Analysis of the tertiary structure of Hsp70 proteins by tryptophan fluorescence
The proteins were excited at 295 nm and the fluorescence emission spectra was monitored at 300 - 400 nm. (A)The recorded tryptophan fluorescence emission spectra for PfHsp70-xF, PfHsp70-xT and hHsp70 proteins. (B) The recombinant PfHsp70-xF, (C) PfHsp70-xT and (D) hHsp70 proteins tryptophan fluorescence emission spectra were recorded under varying urea concentrations. The shift in emission spectra of the proteins exposed to variable urea concentrations were also derived (E).

3.6. The suppression of heat-induced aggregation of malate dehydrogenase (MDH) by PfHsp70-xF, PfHsp70-xT and hHsp70

The ability of the three Hsp70 proteins to suppress heat-induced aggregation of model substrate MDH was investigated by observing the change in turbidity of the reaction mixtures at 340 nm. MDH aggregation in the absence of chaperones was monitored at 51 °C and set as MDH aggregation (Figure 3.8A, B and C). The preparations of PfHsp70-xF, PfHsp70-xT and hHsp70 proteins displayed stability at 51 °C (Figure 3.8A, B and C, respectively). The relative aggregation percentage of the reaction mixtures were determined based on data obtained from

assay in which MDH was analyzed in the absence of a chaperone. BSA (negative control) was not able suppress the aggregation of MDH (Figure 3.8D).

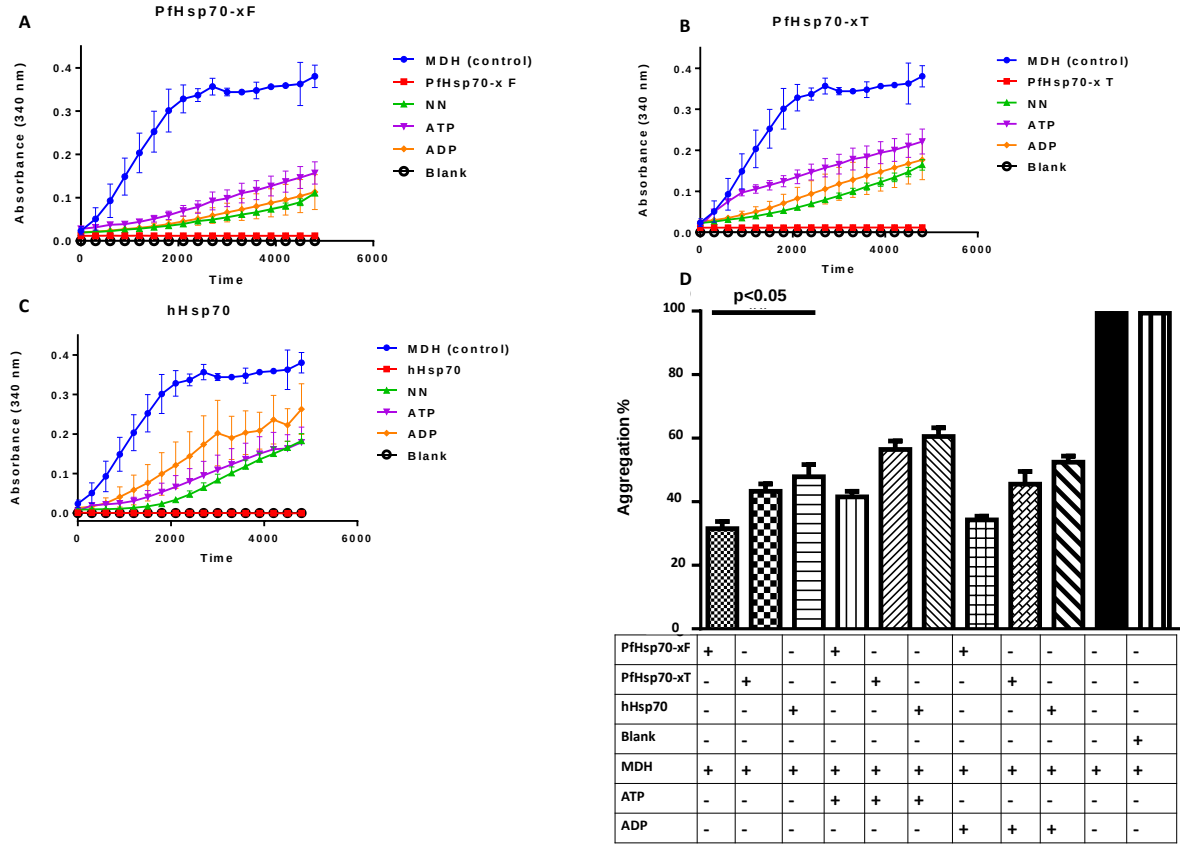

Figure 3.8. Hsp70s suppress heat-induced aggregation of malate dehydrogenase
The heat-induced aggregation of model substrate MDH at 51 °C was spectroscopicaly monitored in vitro at 340 nm. The ability of PfHsp70-xF, PfHsp70-xT and hHsp70 proteins to suppress heat-induced aggregation of model substrate MDH (A, B and C) in the absence of nucleotides (NN), in the presence of ATP (ATP) and in the presence of ADP (ADP) was shown. There was significant difference in the aggregation suppression of PfHsp70-xF, PfHsp70-xT and hHsp70 (D). The addition of 5 µM ADP and 5 µM ATP did not significantly change the ability of chaperones in suppression. Standard deviations as shown by error bars were obtained from three independent replicate assays. GraphPad prism 6.05 was used to conduct ANOVA to determine the significance of the differences.

PfHsp70-xF, PfHsp70-xT and hHsp70 proteins were able to suppress the aggregation MDH. PfHsp70-xF protein showed significantly higher ability to suppress the model substrate than hHsp70 protein (Figure 3.8D, $p < 0.05$). Furthermore, the effect of nucleotides on the ability of PfHsp70-xF, PfHsp70-xT and hHsp70 to suppress the aggregation of MDH respectively was assessed (Figure 3.8A, B, C and D). The presence of ADP did not affect the ability of hHsp70, PfHsp70-xF and PfHsp70-xT to suppress the model substrate this is in agreement with a previous study by (Mabate, 2017) (Figure 3.8 D). However, the addition of ATP lowered the ability of PfHsp70-xF, PfHsp70-xT and hHsp70 to suppress MDH aggregation (Figure 3.8D, $p < 0.05$).

3.7. Slot blot analysis of interaction of PfHsp70-x and hHsp70 with Human GrB

The direct interaction of the recombinant Hsp70 proteins with GrB was confirmed using slot blot assay. The test proteins and control proteins were immobilized onto nitrocellulose membrane using slot blotting (Zininga *et al*., 2016). Varying concentrations (5 µg, 10 µg and 20 µg) of the recombinant proteins PfHsp70-xF, PfHsp70-xT and hHsp70 were immobilized onto a nitrocellulose membrane (Figure 3.9A).

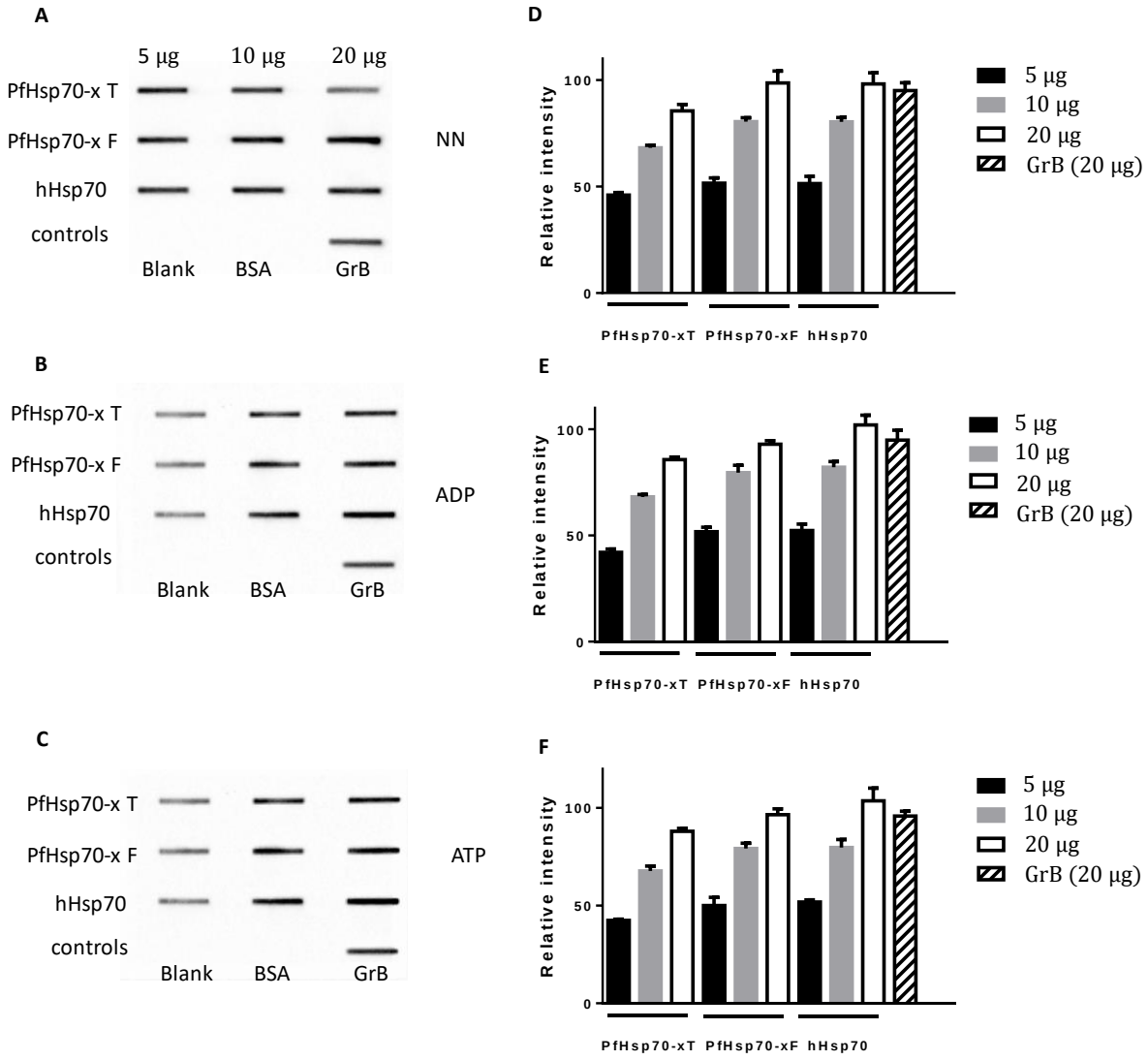

Figure 3.9. Slot Blot confirmation of the direct interaction between Granzyme B and Hsp70s
Interaction between the immobilized bait proteins (PfHsp70-xF, PfHsp70-xT and hHsp70) and the prey protein was detected using α-GrB (A). The experiment was repeated in the presence of nucleotides (B and C) and furthermore the relative intensity of the bands obtained in each blot was measured using the BioRad Image Lab™ software (D, E and F).

In addition, 20 µg of the negative control (BSA) and positive control (GrB) were immobilized in the control-lane (Figure 3.9A). Interaction of the bait protein with the prey protein (GrB) and was confirmed by probing with α-GrB antibody and the relative intensity of the signal was

quantified by densitometry (Figure 3.9A and D). The assay was repeated in the presence nucleotides (5 mM ATP/ADP). The nucleotides did not significantly affect the interaction of GrB with the Hsp70 proteins (Figure 3.9B, C, E and F).

3.8. Investigation of direct interaction between Hsp70s and human GrB using ELISA analysis

In addition to slot blot analysis, ELISA was conducted to confirm the association of PfHsp70-xF/PfHsp70-xT and human Hsp70 with human GrB. The ELISA was based on a previously described protocol by (Biesiadecki and Jin., 2011). The direct protein-protein interaction of the PfHsp70-xF/PfHsp70-xT and human Hsp70 proteins with GrB was concentration dependent indicating that the interactions were specific (Appendix B: Figure B3). The assay was repeated in the presence of 5 mM ATP/ADP. The ELISA result showed that the interaction of GrB with PfHsp70-xF/PfHsp70-xT and human Hsp70 proteins is concentration dependent both in the presence of nucleotides and in their absence. BSA was used as a control and did not interact with the GrB protein. This further suggests that interaction of GrB with Hsp70 was specific as the presence of Hsp70 as bait was required for the association to take place.

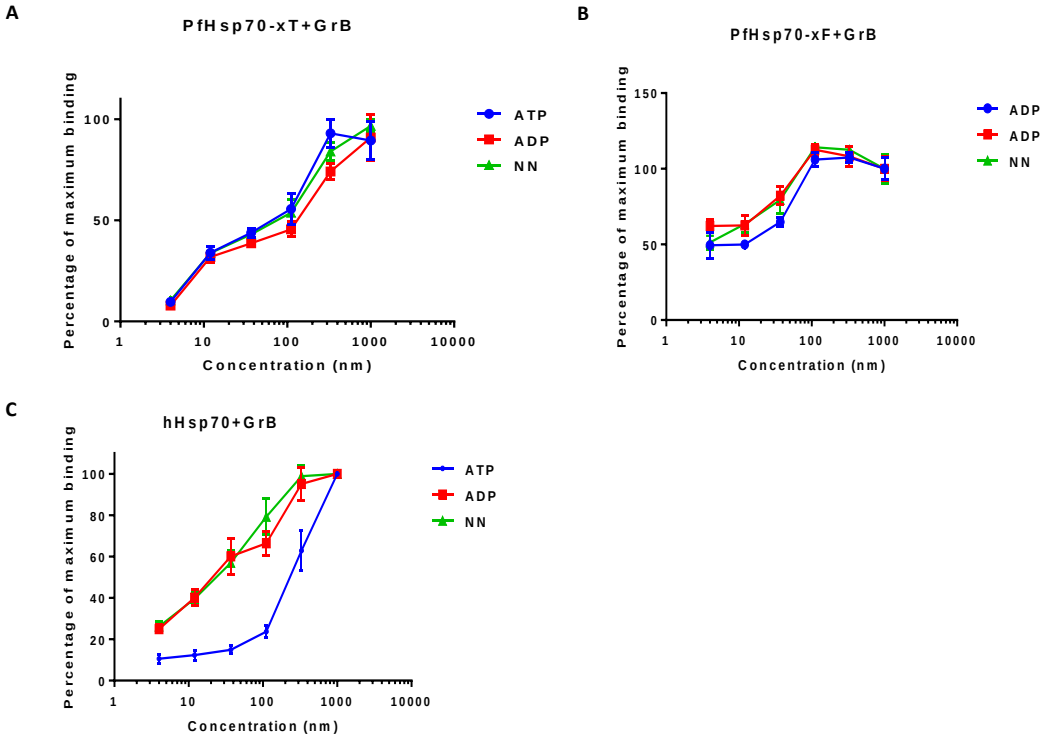

Figure 3.10. The interactions of PfHsp70-xF/PfHsp70-xT and hHsp70 with GrB are concentration dependent
Titration curves for the association of human GrB with PfHsp70-x and hHsp70 were also generated. The curves allowed the analysis of the effect of nucleotides on the PfHsp70-xF-GrB association (A), PfHsp70-xT-GrB association (B) and hHsp70-GrB association(C). The associations of GrB with the Hsp70 proteins were subjected to the presence of nucleotides ATP, ADP and NN-absence of nucleotides.

The data was then used to plot titration curves against a log scale of the dilution concentrations (Figure 3.10 A, B and C). The curves were fitted to determine approximate representative equilibrium binding constant (Kd) for each of the interactions (Table 3.1).

To further validate the interaction, the respective titration curves provided approximate information on interaction kinetics and affinity (Table 3.1). The full-length parasite protein (PfHsp70-xF) exhibited higher affinity for GrB than human Hsp70 protein (Table 3.1). The same phenomena were observed in the presence of nucleotides. However, the truncated form of the parasite protein (PfHsp70-xT) possessed the lowest affinity for its interaction with GrB. The interaction of PfHsp70-xF and hHsp70 with GrB were affected by the presence of ATP which lowers their respective binding affinities (Table 3.1).

Table 3.1. Binding kinetics of the interaction of GrB with PfHsp70-xF/PfHsp70-xT and hHsp70

Ligand	Analyte	Nucleotides	Kd/ nM (± SD)	R^2
PfHsp70-xF	GrB	-	6.46 (± 0.1)	0.91
		5 mM ADP	4.43 (± 0.1)	0.86
		5 mM ATP	9.59 (± 0.2)	0.89
PfHsp70-xT	GrB	-	44.00 (± 9,3)	0.81
		5 mM ADP	38.38 (± 8,8)	0.75
		5 mM ATP	51.25 (± 13,6)	0.70
hHsp70	GrB	-	20.79 (± 0.3)	0.93
		5 mM ADP	19.20 (± 0.4)	0.88
		5 mM ATP	441.80 (± 95,3)	0.95

Table legends: *Kd* equilibrium binding constant, SD- standard deviation, R^2-quantifies the goodness of fit

3.9. The interaction of GrB with PfHsp70-x and hHsp70 occurs through their respective TKD motifs

To confirm that the interactions of GrB with PfHsp70-x and hHsp70 occur through their TKD motifs an additional ELISA assay was conducted. Synthetic peptides representing the TKD motifs of PfHsp70-x and hHsp70 were immobilized onto the wells, while GrB was used as the analyte (Figure 3.11). The concentration dependence of the respective interaction was demonstrated, indicating that the interaction was specific (Figure 3.11A and B). Titration curves were then plotted for each of the interactions which were fitted to acquire binding affinities (Figure 3.11C).

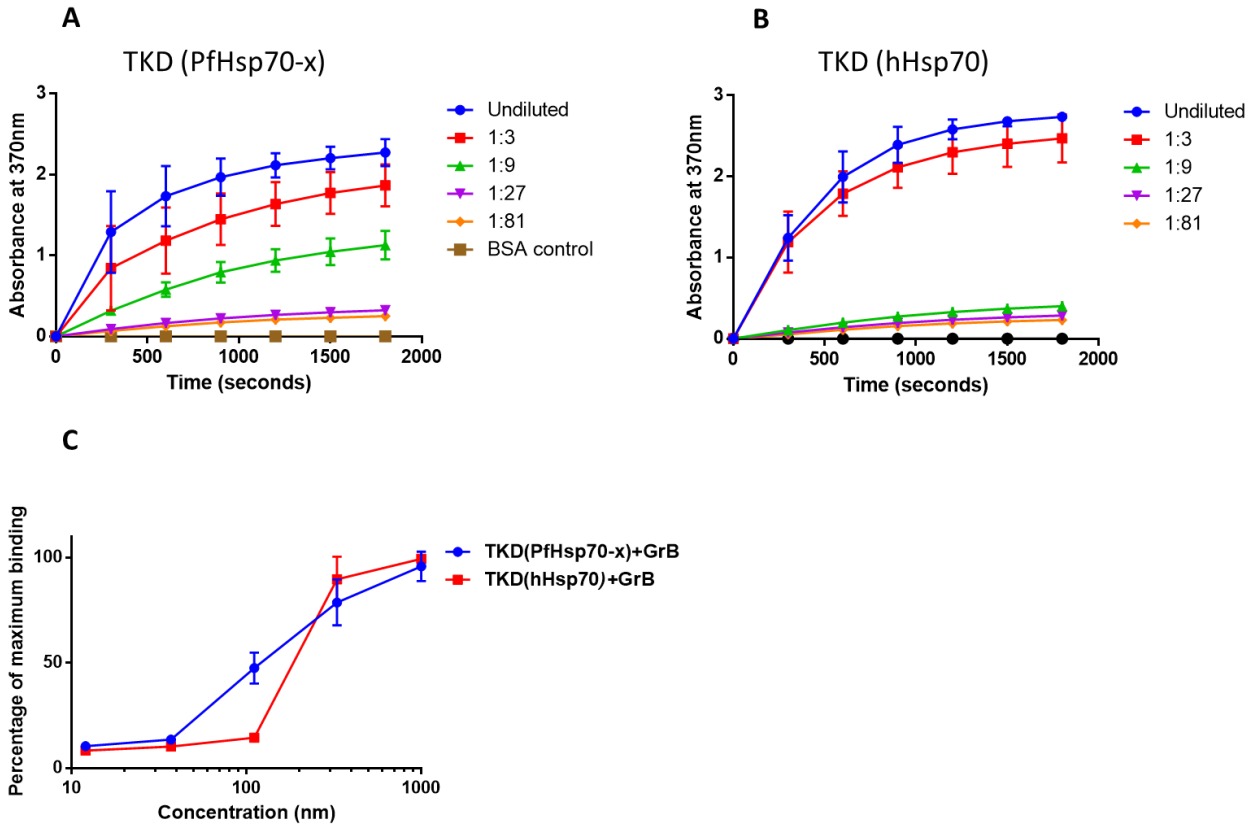

Figure 3.11. The interactions of GrB with PfHsp70-x and hHsp70 occur through the TKD motif
The representative interaction curves generated from the ELISA analysis of PfHsp70-x TKD-GrB association (A) and hHsp70 TKD-GrB association (B). The resulting titration curves against a log scale of the dilution concentrations (C).

In addition, the acquired Kd values allowed a comparison between the affinities of the TKD motifs of parasite and human origin. The parasite TKD showed greater affinity for human GrB than the human TKD (Table 3.2), this validates the previous data set (Table 3.1).

Table 3.2. The interaction of GrB with parasite TKD and human TKD motifs

Ligand	Analyte	Kd/ nM (± SD)	R^2
TKD (PfHsp70-x)	GrB	165.9 (± 29,05)	0.96
TKD (hHsp70)	GrB	349.4 (± 136,80)	0.88

Table legends: *Kd* equilibrium binding constant, SD- standard deviation, R^2-quantifies the goodness of fit

3.10. Investigation of the effect of human GrB on parasite growth

The ability of human GrB to inhibit parasite growth was investigated by monitoring the activity of lactate dehydrogenase (pLDH) of *P. falciparum* 3D7 cultured in vitro, as previously described (Makler *et al.*, 1993; Zininga *et al.*, 2017). The antimalarial compound chloroquine was exposed to the parasites as a positive control which inhibited parasite growth by 50 % (IC50) at a final concentration of 8.5 nM (Figure 3.12). The inhibition of parasite growth in the

presence of GrB occurred in a concentration-dependent manner (Figure 3.12). GrB inhibited 50% of parasite growth (IC50) at a concentration of 0.546 µM.

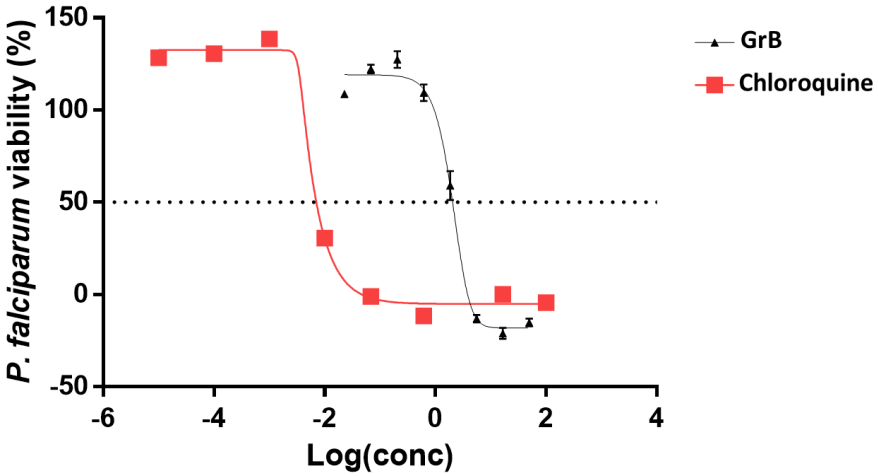

Figure 3.12. The n vitro susceptibility of *P. falciparum* to GrB represented as normalized dose response curve

The curves represent data obtained from assays conducted in the presence of chloroquine (IC50 of 0.0085 µM) or GrB (IC50 of 0.546 µM), respectively. IC50 values were calculated from the generated dose response curves obtained using GraphPad Prism 6. The experiment was performed in duplicate. Standard deviations obtained from three replicate assays are shown.

4. Discussion and Conclusion

Out of the six Hsp70s expressed by *P. falciparum*, PfHsp70-x is exported to the erythrocyte cytosol and cell membrane (Külzer *et al*., 2012). Although the function of PfHsp70-x is unclear, it has been shown to associate with other exported parasite proteins such as Hsp40s of *P. falciparum* origin exported to the erythrocyte and the virulence factor PfEMP1 (Külzer *et al*., 2012; Zhang *et al*., 2017). PfHsp70-x has been implicated in trafficking of parasite proteins to the erythrocyte as it also associates with components of the PTEX translocon (Zhang *et al*., 2017). Interestingly, PfHsp70-x is dispensable at the erythrocyte stage of the parasite cultured in vitro (Cobb *et al*., 2017; Charnaud *et al*., 2017). However, the presence of PfHsp70-x on the erythrocytes cell surface suggests an important role for this protein which may not yet be fully understood. Interestingly, previous studies in cancer have shown that human Hsp70s have immunomodulatory function through their interaction with human GrB produced by NK cells (Gross *et al*., 2003). The interaction occurs through a 14-amino acid Hsp70 sequence, the TKD motif, which directly interacts with the human GrB (Gross *et al*., 2003; Multhoff., 2007). PfHsp70-x also contains the TKD motif, therefore this study sought to confirm the direct interaction between human GrB with PfHsp70-x/ hHsp70.

The recombinant forms of PfHsp70-xF, PfHsp70-xT and hHsp70 were expressed in *E. coli* BL21 (DE3) cells. PfHsp70-xF, PfHsp70-xT and hHsp70 were successfully expressed (Figure 3.3A and B; Figure 3.4A, respectively). Leaky expression was observed before induction with IPTG. This was expected as this was also reported in previous studies (Mabate, 2017; Monyai, 2018). Leaky expression is a result of unregulated *lac* promoters (T5 promoter of pQE30 vector based constructs (Rosano and Ceccarelli, 2014).

The expressed parasite recombinant proteins PfHsp70-xF and PfHsp70-xT were purified from the soluble fractions (Figure 3.4). Protein yields of approximately 6 mg/l and 4 mg/l for PfHsp70-xF and PfHsp70-xT respectively were achieved. The yield was considerably higher than the yield of approximately 1 mg/l previously obtained by Mabate (2017) but is within the previously obtained range of approximately 4- 8 mg/l of the culture reported by Cockburn *et al* (2014). The recombinant hHsp70 protein was also successfully purified resulting in a yield of 11 mg/l.

The secondary structures of PfHsp70-xF, PfHsp70-xT and hHsp70 were evaluated and the stability of each protein was determined by urea treatment. For all three proteins the far-UV spectra showed a positive peak at around 190 nm and two troughs at 209 and 221 nm,

respectively (Figure 3.6A). The recombinant proteins were predominantly α-helical in character, similar to previously obtained data (Mabate, 2017). Of the three proteins, PfHsp70-xF was relatively more stable, as it maintained conformation in the presence of up to 2 M urea and gradually unfolded in the presence of less than 4 M urea. However, at higher urea concentration, it drastically lost its conformation (Figure 3.6B). Of the three proteins, PfHsp70-xT was the least stable. The stability of PfHsp70-x to heat stress (Figure 3.8) relates to the need for it to remain functionally viable at elevated temperatures associated with malaria fever. In addition, the difference in the stability of PfHsp70-xF and PfHsp70-xT to stress shows the importance of the EEVN motif in the protein's functionality and stability as previously reported (Mabate *et al*., 2018).

Furthermore, the tertiary structure of PfHsp70-xF, PfHsp70-xT and hHsp70 was analysed using tryptophan fluorescence spectroscopy (Figure 3.7). Increase in urea concentration resulted in reduced tryptophan fluorescence signal, suggesting quenching of the relative fluorescence dependent on urea concentration (Figure 3.7B, C and D). Both PfHsp70-xF and PfHsp70-xT exhibited tryptophan fluorescence conformational changes which registered a red shift implying that the tryptophan residues were more exposed in response to presence of urea, confirming denaturation/unfolding of the proteins (Figure 3.7E; Zininga, 2015). However, the hHsp70 showed a blue shift suggesting that the protein's tryptophan residues became hidden with increase in urea concentration (Figure 3.7E). This is likely due to the fact that hHsp70 aggregated in response to exposure to urea, thereby burying its tryptophan residues.

The ability to suppress heat-induced aggregation of model substrate (MDH) by PfHsp70-xF, PfHsp70-xT and hHsp70 was investigated. The three proteins did not aggregate when subjected to a temperature of 51 °C, showing their resistance to heat stress. Furthermore, all three proteins successfully suppressed MDH aggregation (Figure 3.8). The effect of nucleotides on respective Hsp70's ability to suppress aggregation was also investigated. The presence of ADP did not affect chaperone activity of PfHsp70-xF and PfHsp70-xT which is in line with previous reports (Figure 3.8 D; Mabate., 2017). On the other hand, the presence of ATP greatly reduced the ability of PfHsp70-xF, PfHsp70-xT and hHsp70 to suppress MDH aggregation (Figure 3.8D, $p < 0.05$). This is a consequence of ATP inhibiting the association of the chaperones with their substrates. It is known that when bound to ATP, Hsp70s possess reduced affinity for the substrate (Buchberger *et al*., 1995). PfHsp70-xF and PfHsp70-xT demonstrated significant suppression of MDH over hHsp70 (Figure 3.8 $p < 0.05$). This further showed that PfHsp70-x is more stable and functionally effective compared to hHsp70.

The study further sought to investigate the interaction of PfHsp70-x and hHsp70 with human GrB. The interaction was confirmed using slot blot assay. Monoclonal α-GrB antibody was used to probe for GrB retention by bait protein (Figure 3.9). All three proteins PfHsp70-xF, PfHsp70-xT and hHsp70 directly interacted with GrB as confirmed by densitometric estimates (Figure 3.9). Furthermore, an ELISA assay was conducted to confirm the slot blot based results. The ELISA showed that the interaction was concentration dependent and stable (Figure 3.10). The approximated kinetics obtained from the ELISA, showed that PfHsp70-xF had three fold greater affinity for binding to human GrB (Table 3.1). The absence of the EEVN motif reduced the affinity for GrB binding to PfHsp70-xT as compared to PfHsp70-xF. In addition, an ELISA assay was conducted to investigate interaction of synthetic peptides representing the Hsp70-TKD motifs with the respective Hsp70 (Figure 3.11). The same phenomena were observed, with the PfHsp70-x TKD motif having greater affinity for binding GrB than hHsp70 (Table 3.2). In addition, the full-length PfHsp70-x and hHsp70 had greater affinities for GrB than their respective TKD motifs. This suggests that other residues flanking the TKD motifs may be involved in the interaction between Hsp70 and GrB. PfHsp70-xT had lower affinity for GrB than PfHsp70-xF, suggesting that the EEVN may facilitate interaction of GrB and Hsp70.

Furthermore, the effect of GrB on parasite growth was also investigated. A culture of *P. falciparum* 3D7-infected erythrocytes was treated with varying amounts of GrB. As a positive control the parasites were exposed to chloroquine which inhibited parasite growth by 50 % (IC50) at a final concentration of 8.5 nM (Figure 3.12). GrB inhibited 50% of parasite growth (IC50) at a concentration of 0.546 µM (Figure 3.12). Despite GrB's ability to inhibit parasite growth, it was much less effective than chloroquine and hence GrB requires further development towards becoming an effective anti-plasmodial drug.

This study has provided evidence for the direct interaction between PfHsp70-x/hHsp70 and human GrB as shown by the results obtained from the ELISA and slot blot assays. It is important to further investigate the interaction using cell based assays such as co-immuno precipitation to validate the interaction.

In conclusion human GrB showed potential as an anti-plasmodial agent. Human GrB provides an option for immune based therapy as an alternative to the traditional chemical entities as antimalarial drugs. Immune based therapy provides the advantage of reduced side effects as GrB is native to the human host. Altogether, the findings from this study suggest that both hHsp70 and PfHsp70-x may facilitate uptake of GrB by erythrocytes leading to eryptosis.

References

Artavanis-Tsakonas, K., Riley, E. M. (2002). Innate immune response to malaria: Rapid induction of IFN- γ from human NK cells by live *Plasmodium falciparum* infected erythrocytes. Journal of Immunology. 169: 2956-2963.

Bannister, L.H. (2001). Looking for the exit: How do malaria parasites escape from red blood cells? Proceedings of the National Academy of Sciences of the United States of America. 98: 383-4.

Bascos, N.A.D., Mayer, M.P., Bukau, B., Landry, S.J. (2017). The Hsp40 J-domain modulates Hsp70 conformation and ATPase activity with a semi-elliptical spring. Protein Science. 26: 1838-1851.

Batinovic, S., Mchugh, E., Chisholm, S. A., Matthews, K., Liu, B., Dumont, L., Charnaud, S., Schneider, M., Gilson, P., de Koning-Ward, T., Dixon, M., Tilley, L. (2017). *Plasmodium* - infected erythrocytes. Nature Communications. 8: 16044.

Biesiadecki, B. J., Jin, J. P. (2011). A high-throughput solid-phase microplate protein-binding assay to investigate interactions between myofilament proteins. Journal of Biomedicine and Biotechnology. 52: 421701.

Billker, O., Shaw, M. K., Margos, G., Sinden, R. E. (1997) The roles of temperature, pH and mosquito factors as triggers of male and female gametogenesis of *Plasmodium berghei* invitro. Parasitology. 115: 1-7.

Boddey, J. A., Moritz, R. L., Simpson, R. J., Cowman, A. F. (2009). Role of the *Plasmodium* export element in trafficking parasite proteins to the infected erythrocyte. Traffic. 10: 285-299.

Banerji, U. (2009). Heat shock protein 90 as a drug target: Some like it hot. Clinical Cancer Research.15: 9-14.

Boshoff, A., Nyakundi, D. O., Bentley, S. J. (2018). Hsp70 escort protein: More than a regulator of mitochondrial Hsp70. Current Proteomics. 16: 64.

Botha, M., Chiang, A.N., Needham, P.G., Stephens, L.L., Hoppe, H.C., Külzer, S., Przyborski, J.M., Lingelbach, K., Wipf, P., Brodsky, J.L., Shonhai, A., Blatch, G.L. (2011). *Plasmodium falciparum* encodes a single cytosolic type I Hsp40 that functionally interacts with Hsp70 and is upregulated by heat shock. Cell Stress and Chaperones. 16: 389-401.

Botha, M., Pesce, E.R., Blatch, G.L. (2007). The Hsp40 proteins of *Plasmodium falciparum* and other apicomplexa: Regulating chaperone power in the parasite and host. The international Journal of Biochemistry and Cellular Biology. 39: 1781-1803.

Böttger, E., Multhoff, G., Kun, J.F.J., Esen, M., (2012). *Plasmodium falciparum* infected erythrocytes induce granzyme B by NK cells through expression of host. Public Library of Science One. 7: e33774.

Boyle, M.J., Richards, J.S., Gilson, P.R., Chai, W., Beeson, J.G. (2010). Interactions with heparin-like molecules during erythrocyte invasion by *Plasmodium falciparum* merozoites. Blood. 115: 4559-68.

Bozdech, Z., Llinás, M., Pulliam, B. L., Wong, E. D., Zhu, DeRisi J. L. (2003) The transcriptome of the intraerythrocytic developmental cycle of *Plasmodium falciparum*. Public Library of Science Biology. 1: 85-100.

Bratke, K., Kuepper, M., Bade, B., (2005). Differential expression of human granzymes A, B, and K in natural killer cells and during CD8 + T cell differentiation in peripheral blood. Journal of Immunology. 35: 2608-2616.

Bukau, B., Horwick, A. L. (1998). The Hsp70 and Hsp60 chaperone machines. Cell. 92: 351-366.

Bukau, B., Weissman, J., Horwich, A. (2006). Molecular chaperones and protein quality control. Cell. 125: 443-451.

Buchberger, A., Theyssen, H., Schröder, H., McCarty, J. S., Virgallita, G., Milkereit, P., Reinstein, J., Bukau, B. (1995). Nucleotide-induced conformational changes in the ATPase and substrate binding domains of the DnaK chaperone provide evidence for interdomain communication. Journal of Biological Chemistry. 270: 16903-16910.

Bullock, W.O., Fernandez, J.M. and Short J.M. (1987). XL1-Blue- a high-efficiency plasmid transforming recA Escherichia coli strain with β-galactosidase selection. Biotechniques. 5: 376-379.

CDC (2012) Malaria parasites (Available from http://www.cdc.gov/malaria/.../parasites.html [accessed on 20 March 2017]).

CDC (2016) Malaria facts. (Available from http://www.cdc.gov/malaria/about/biology [accessed on 25 March 2017]).

Chang, H.H., Falick, A.M., Carlton, P.M., Sedat, J.W., DeRisi, J.L., Marletta, M.A. (2008). N-terminal processing of proteins exported by malaria parasites. Molecular and Biochemical Parasitology.160: 107-115.

Charnaud, S. C., Dixon, M. W. A., Nie, C. Q., Chappell, L., Sanders, P. R., Nebl, T., Hanssen, E., Berriman, M., Chan, J., Blanch, A., Beeson, J., Rayner, J., Przyborski, J., Tilley, L., Crabb, B., Gilson, P. R. (2017). The exported chaperone Hsp70-x supports virulence functions for *Plasmodium falciparum* blood stage parasites. Public Library of Science One. 12: e0181656.

Chen, Q., Amaladoss, A., Ye, W., Liu, M., Dummler, S., Kong, F., Hiong, L. (2014). Human natural killer cells control *Plasmodium falciparum* infection by eliminating infected. Immunology. 111: 1479-1484.

Cockburn, I. L, Boshoff, A, Pesce, E and Blatch, G. L. (2014). Selective modulation of Plasmodial Hsp70s by small molecules with anti-malarial activity. Biological Chemistry. 395: 1437-4315.

Cockburn, I.L. (2012) Modulation of *Plasmodium falciparum* chaperones PfHsp70-1 and PfHsp70-x by small molecules (Doctoral dissertation). Available at https://core.ac.uk/download/pdf/145040454.pdf

Cobb, D. W., Florentin, A., Fierro, M. A., Krakowiak, M., Moore, J. M., Muralidharan, V. (2017). The exported chaperone PfHsp70x is dispensable for the *Plasmodium falciparum* intraerythrocytic life cycle. MSphere. 2: e00363-17.

Cox, F.E. (2010). History of the discovery of the malaria parasites and their vectors. Parasites and Vectors. 3: 5.

Crompton, P. D., Pierce, S. K., Miller, L. H. (2010) Advances and challenges in malaria vaccine development. Journal of Clinical Investigation. 120: l 4168-78.

Crabb, B. S., Koning-ward, T. F. De, Gilson, P. R. (2010). Protein export in Plasmodium parasites: From the endoplasmic reticulum to the vacuolar export machine. International Journal for Parasitology. 40: 509–513.

Cui, J., Ma, C., Ye, G., Shi, Y., Xu, W., Zhong, L. (2017). DnaJ (hsp40) of *Streptococcus pneumoniae* is involved in bacterial virulence and elicits a strong natural immune reaction via PI3K / JNK. Molecular Immunology. 83: 137-146.

Cui, L., Su, X. (2009). Discovery, mechanisms of action and combination therapy of artemisinin. Expert Review of Anti-infective Therapy. 7: 999-1013.

Cui, L., Mharakurwa, D.N., Ndiaye, D., Rathod, P.K., Rosenthai, P.J. (2015). Antimalarial drug resistance: Literature review and activities and findings of the ICEMR Network. American Journal of Tropical Medicine and Hygene. 93: 57-68.

Dalod, M., Chelbi, R., Malissen, B., and Lawrence, T. (2014). Dendritic cell maturation: functional specialization through signaling specificity and transcriptional programming. European Molecular Biology Organization Journal. 33: 1104-1116.

de Poot, S. A., Bovenschen, N. (2014). Granzyme M: behind enemy lines. Cell death and differentiation. 21: 359-68.

Dragovic, Z., Broadley, S.A., Shomura, Y., Bracher, A., Hartl, F.U. (2006). Molecular chaperones of the Hsp110 family act as nucleotide exchange factors of Hsp70s. European Molecular Biology Organization Journal. 25: 2519-2528.

Eaton, P., Zuzarte-Luis, V., Mota, M.M., Santos, N.C., Prudêncio, M. (2012). Infection by *Plasmodium* changes shape and stiffness of hepatic cells. Nanomedicine. 8: 17-9.

Edkins, A.L., Boshoff, A. (2014). Gereneral structural and functional features of molecular chaperones. In: Shonhai, A., Blatch, G. Editors. Heat shock proteins of malaria. Springer, Dordrecht. 5-45.

Eliseo, D. D., Rocco, G. Di, Loria, R., Soddu, S., Santoni, A., Velotti, F. (2016). Epithelial to mesenchimal transition and invasion are upmodulated by tumor- expressed granzyme B and inhibited by docosahexaenoic acid in human colorectal cancer cells. Journal of Experimental and Clinical Cancer Research. 35: 24.

Evans, C.G., Chang, L., Gestwicki, J.E. (2010). Heat shock protein 70 (hsp70) as an emerging drug target. Journal of Medicinal Chemistry. 53: 4585-4602.

Goeckeler, J.L., Stephens, A., Lee, P., Caplan, A.J., Brodsky, J.L. (2002). Overexpression of yeast Hsp110 homolog Sse1p suppresses ydj1-151 thermosensitivity and restores Hsp90-dependent activity. Molecular Biology of the Cell Journal. 13: 2760-2770.

Gregson, A., Plowe, C. V. (2005). Mechanisms of resistance of malaria parasites to antifolates. Pharmacological Reviews. 57: 117-145.

Gross, C., Koelch, W., Demaio, A., Arispe, N., Multhoff, G. (2003). Cell surface-bound heat shock protein 70 (Hsp70) mediates perforin-independent apoptosis by specific binding and uptake of granzyme B. Journal of Biological Chemistry. 278: 41173-41181.

Hartl, F.U. (1996). Molecular chaperones in cellular protein folding. Nature. 381: 571–580.

Hennessy, F., Nicoll, W.S., Zimmermann, R., Cheetham, M.E., Blatch, G.L. (2005). Not all J domains are created equal: Implications for the specificity of Hsp40-Hsp70 interactions. Protein Science. 14: 1697-1709.

Hiss, J. A., Przyborski, J. M., Schwarte, F., Lingelbach, K., Schneider, G. (2008). The *Plasmodium* export element revisited. Public Library of Science One. 3: e1560.

Hiller, N.L., Bhattacharjee, S., van Ooij, C., Liolios, K., Harrison, T., Lopez-Estrano, C., Haldar, K. (2004). A host targeting signal in virulence proteins reveals a secretome in malarial infection. Science. 306: 1934-1937.

Ida, H., Utz, P. J., Anderson, P. (2005). Granzyme B and natural killer (NK) cell death. Modern Rheumatology. 15: 315-322.

Joly, A. L., Wettstein, G., Mignot, G., Ghiringhelli, F., Garrido, C. (2010). Dual role of heat-shock proteins as regulator of apoptosis and innate immunity. Journal of Innate Immunity. 2: 238-247.

Kampinga, H. H., Craig, E. A. (2010). The Hsp70 chaperone machinery: J-proteins as drivers of functional specificity. Nature Reviews. Molecular Cell Biology. 11: 579-592.

Kampinga, H. H., Hageman, J., Vos, M. J., Kubota, H., Tanguay, R. M., Bruford, E., Cheetham, M.E., Chen, B., Hightower, L. E. (2009). Guidelines for the nomenclature of the human heat shock proteins. Cell Stress and Chaperones. 14: 105-111.

Kim, Y. E., Hipp, M. S., Bracher, A., Haye-Hartl, M., Hartl, F. U. (2013). Molecular chaperone functions in protein folding and proteostasis. Annual Review of Biochemistry. 82: 323-355.

Kityk, R., Kopp, J., Sinning, I., Mayer, M. P. (2012). Structure and dynamics of the ATP-bound open conformation of Hsp70 chaperones. Molecular Cell. 48: 863-874.

Külzer, S., Charnaud, S., Dagan, T., Riedel, J., Mandal, P., Pesce, E.R., Blatch, G.L., Crabb, B.S., Gilson, P.R., Przyborski, J.M. (2012). *Plasmodium falciparum*-encoded exported

Hsp70/Hsp40 chaperone/co-chaperone complexes within the host erythrocyte. Cellular Microbiology. 14: 1784-1795.

Külzer, S., Rug, M., Brinkmann, K., Cannon, P., Cowman, A., Lingelbach, K., Blatch, G.L., Maier, A.G., Przyborski, J.M. (2010). Parasite-encoded Hsp40 proteins define novel mobile structures in the cytosol of the *P. falciparum*-infected erythrocyte. Cellular Microbiology. 12: 1398-1420.

Lasonder, E., Janse, C.J., van Gemert, G.J., Mair, G.R., Vermunt, A.M., Douradinha, B.G., van Noort, V., Huynen, M.A., Luty, A.J., Kroeze, H., Khan, S.M., Sauerwein, R.W., Waters, A.P., Mann, M., Stunnenberg, H.G. (2008). Proteomic profiling of *Plasmodium* sporozoite maturation identifies new proteins essential for parasite development and infectivity. Public Library of Science Pathogens. 4: e1000195.

Li, J., Qian, X. Sha, B. (2009). Heat shock protein 40: structural studies and their functional implications. Protein and Peptide Letters. 16: 606-612.

Li, Z., Srivastava, P. (2004) Heat shock proteins. Current Protocols in Immunology. 10: 1002-1011.

Lindquist, S. And Craig, E.A. (1988). The heat shock proteins. Annual Review of Genetics. 22: 631-677.

Mabate, B. (2017). Exploration of interaction between *Plasmodium falciparum* Hsp70-x (PfHsp70-x) and human Hsp70-Hsp90 organizing protein (human Hop) (Masters dissertation). Available at http://univendspace.univen.ac.za/handle/11602/934. (Accessed June 2017).

Mabate, B., Zininga, T., Ramatsui, L., Makumire, S., Achilinou, I., Dirr, H., Shonhai, A. (2018). Structural and biochemical characterization of *Plasmodium falciparum* Hsp70-x reveals functional versatility of its C-terminal EEVN motif. Proteins: Structure Function and Bioinformatics. 86: 1189-1201.

Makler, M.T., Ries, J.M., Williams, J.A., Bancroft, J.E., Piper, R.C., Gibbins, B.L., Hinrichs, D.J. (1993). Parasite lactate dehydrogenase as an assay for *Plasmodium falciparum* drug sensitivity. American Journal of Tropical Medicine and Hygiene. 48: 739-741.

Maier, A. G., Rug, M., O'Neill, M. T., Brown, M., Chakravorty, S., Szestak T., Chesson J., Wu Y., Hughes K., Coppel, R. L., Newbold, C., Beeson, J. G., Craig, A., Crabb, B. S.,

Cowman, A. F. (2008). Exported proteins required for virulence and rigidity of *Plasmodium falciparum* infected human erythrocytes. Cell. 134: 48-61.

Marti, M., Good, R.T., Rug, M., Knuepfer, E., Cowman, A.F. (2004). Targeting malaria virulence and remodeling proteins to the host erythrocyte. Science. 306: 1930-1933.

Matthews, K., Kalanon, M., Chisholm, S. A., Sturm, A., Goodman, C. D., Dixon, M. W. A., Sanders, P.R., Nebl, T., Fraser, F., Haase, S., McFadden, G.I., Gilson, P. R., Crabb, B. S., De Koning-Ward, T. F. (2013). The *Plasmodium* translocon of exported proteins (PTEX) component thioredoxin-2 is important for maintaining normal blood-stage growth. Molecular Microbiology. 89: 1167–1186.

Mayer, M.P. (2013). Hsp70 chaperone dynamics and molecular mechanism. Trends in Biochemical Sciences. 38: 507-514.

Mayer, M. P., Bukau, B. (2005). Cellular and molecular life sciences Hsp70 chaperones: Cellular functions and molecular mechanism. Cellular and Molecular Life Sciences. 62: 670-684.

Mavoungou, E., Luty, A.J., Kremsner, P.G. (2003). Natural killer (NK) cell- mediated cytolysis of *Plasmodium falciparum* infected human red blood cells in vitro. European Cytokine Network. 14: 134-142.

Metkar, S. S., Wang, B., Ebbs, M. L., Kim, J. H., Lee, Y. J., Raja, S. M., & Froelich, C. J. (2003). Granzyme B activates procaspase-3 which signals a mitochondrial amplification loop for maximal apoptosis. Journal of cell biology, 160(6), 875-85.

Menard, D., Dondorp, A. (2017). Antimalarial Drug Resistance: A Threat to Malaria Elimination. Cold Spring Harbor Laboratory Press. 7: a025619.

Multhoff, G. (2007). Heat shock protein 70 (Hsp70): Membrane location, export and immunological relevance. Methods. 43: 229–237.

Multhoff, G., Pockley, A. G., Schmid, T. E., and Schilling, D. (2015). The role of heat shock protein 70 (Hsp70) in radiation-induced immunomodulation. Cancer Letters. 368: 179-184

Miotto, O., Amato, R., Ashley, E. A., Macinnis, B., Almagro-garcia, J., Amaratunga, C., Kwiatkowski, D. P. (2015). Genetic architecture of artemisinin-resistant *Plasmodium falciparum*. Nature Genetics. 47: 226-234

Misra, G., Ramachandran, R. (2009). Hsp70-1 from *Plasmodium falciparum*: protein stability, domain analysis and chaperone activity. Biophysical Chemistry. 142: 55-64.

Monyai, S. F. (2018). Establishment of interaction partners of Plasmodium falciparum heat shock protein 70-x (PfHsp70-x) (Masters dissertation). Available at http://univendspace.univen.ac.za/handle/11602/1113.

Morrissette, N. S and Sibley, L. D. (2002) Cytoskeleton of apicomplexan parasites. Microbiology and Molecular Biology Reviews. 66: 21-38.

Muralidharan, V., Oksman, A., Pal, P., Lindquist, S., Goldberg, D.E. (2012). *Plasmodium falciparum* heat shock protein 110 stabilizes the asparagine repeat-rich parasite proteome during malarial fevers. Nature Communications. 3: 1310.

Njunge, J. M., Ludewig, M. H., Boshoff, A., Pesce, E. R., Blatch, G. L. (2013). Hsp70s and J proteins of *Plasmodium* parasites infecting rodents and primates: Structure, function, clinical relevance, and drug targets. Current Pharmaceutical Design. 19: 387-403.

Oh, H.J., Eston, D., Murawski, M., Kaneneko, Y., Subjeck, J.R., (1999). The chaperoning activity of Hsp110: Identification of functional domains by use of targeted deletions. The Journal of Biological Chemistry. 27: 15712-15718.

Pasvol, G. (2006). The treatment of complicated and severe malaria. British Medical Bulletin. 75-76: 29-47.

Petersen, W., Külzer, S., Engels, S., Zhang, Q., Ingmundson, A., Rug, M., Maier A.G., Przyborski, J. M. (2016). J-dot targeting of an exported Hsp40 in *Plasmodium falciparum*-infected erythrocytes. International Journal for Parasitology. 46: 519-525.

Pettersen, E. F., Goddard, T. D., Huang, C. C., Couch, G. S., Greenblatt, D. M., Meng, E. C., Ferrin, T. E. (2004). UCSF Chimera--a visualization system for exploratory research and analysis. Journal Computational Chemistry 25: 1605-12.

Pesce, E. R., Acharya, P., Tatu, U., Nicoll, W. S., Shonhai, A., Hoppe, H. C., Blatch, G. L. (2008). The *Plasmodium falciparum* heat shock protein 40, Pfj4, associates with heat shock protein 70 and shows similar heat induction and localization patterns. Journal of Biochemistry and Cell Biology. 40: 2914-2926.

Pesce, E.R., Cockburn, I.L., Goble, J.L., Stephens, L.L., Blatch, G.L. (2010). Malaria heat shock proteins: drug targets that chaperone other drug targets. Infectious Disorders - Drug Targets. 10: 147-57.

Pfanner, N., Wiedemann, N. (2002). Mitochondrial protein import: two membranes, three translocases. Current Opinion in Cell Biology. 14: 400-11.

Pallarès, I., de Groot, N. S., Iglesias, V., Sant'Anna, R., Biosca, A., Fernàndez-Busquets, X., & Ventura, S. (2018). Discovering putative prion-like proteins in *Plasmodium falciparum*: A computational and experimental analysis. Frontiers in microbiology. 9: 1737.

Przyborski, J. M., Diehl, M., Blatch, G. L. (2015). Plasmodial Hsp70s are functionally adapted to the malaria parasite life cycle. Frontiers in Bioscience. 2: 34.

Qiu, X.-B., Shao, Y.-M., Miao, S., Wang, L. (2006). The diversity of the DnaJ/Hsp40 family, the crucial partners for Hsp70 chaperones. Cellular and Molecular Life Sciences. 63: 2560-2570.

Radons, J. (2016). The human HSP70 family of chaperones: where do we stand? Cell Stress and Chaperones. 21: 379-404.

Rampelt, H., Mayer, M.P., Bukau, B. (2018). Nucleotide exchange factors for Hsp70 chaperones. In: Calderwood, S., Prince, T. Editors. Molecular chaperones. Methods in Molecular Biology. 787: 83-91.

Roetynck, S., Baratin, M., Vivier, É., Ugolini, S. (2006). Natural killer cells and innate immunity against malaria. Medicine Sciences. 22: 739-44.

Rosano, G.L., Ceccarelli, F.A. (2014). Recombinant protein expression in *E. coli*: advances and challenges. Frontiers in Microbiology. 5: 172.

Rousalova, I., Krepela, E. (2010). Granzyme B-induced apoptosis in cancer cells and its regulation. International Journal of Oncology. 37: 1361-1378.

Raviol, H., Sadlish, H., Rodriguez, F., Mayer, M. P., Bukau, B. (2006). Chaperone network in the yeast cytosol: Hsp110 is revealed as an Hsp70 nucleotide exchange factor. European Molecular Biology Organization Journal. 25: 2510-2518.

Rhiel, M., Bittl1, V., Tribensky, A., Charnaud, S. C., Strecker, M., Müller, S., Lanzer, M., Sanchez, C., Külzer, S., Przyborski, J. M. (2016). Trafficking of the exported *P. falciparum* chaperone PfHsp70- x. Scientific Reports. 6: 36174.

Rowe, J. A., Claessens, A., Corrigan, R. A. (2009). Adhesion of *Plasmodium falciparum* - infected erythrocytes to human cells: molecular mechanisms and therapeutic implications. Expert Reviews in Molecular Medicine. 11: e16.

Saibil, H. (2013). Chaperone machines for protein folding, unfolding and disaggregation. Nature Reviews Molecular Cell Biology. 14: 630-642.

Sedelies, K. A., Sayers, T. J., Edwards, K. M., Chen, W., Pellicci, D. G., Godfrey, D. I., Trapani, J. A. (2004). Discordant regulation of granzyme H and granzyme B expression in human lymphocytes. Journal of Biological Chemistry. 279: 26581-26587.

Shaner, L., Trott, A., Goeckeler, J.L., Brodsky, J.L., Morano, K.A. (2004). The function of the yeast molecular chaperone Sse1 is mechanistically distinct from the closely related Hsp70 family. Journal of Biological Chemistry. 279: 21992-22001.

Sharma, YD., Masison, D.C. (2009). Hsp70 structure, function, regulation and influence on yeast prions. Protein and Peptide Letters. 16: 571-81.

Shonhai, A. (2014). Role of Hsp70s in development and pathogenicity of *Plasmodium* species: In: Shonhai A, Blatch G. Editors. Heat shock proteins of malaria. Springer New York. 47-70.

Shonhai, A., Botha, M., de Beer, T.A.P., Boshoff, A., Blatch, G.L. (2008). Structure-function study of *Plasmodium falciparum* Hsp70 using three-dimensional modelling and in-vitro analyses. Protein and Peptide Letters. 15: 1117-1125.

Shonhai, A., Boshoff, A., Blatch, G.L. (2007). The structural and functional diversity of Hsp70 proteins from *Plasmodium falciparum*. Protein Science. 16: 1803-1818.

Shonhai, A. (2010). Plasmodial heat shock proteins: targets for chemotherapy. Immunology and medical microbiology. 58: 61-74.

Shonhai, A., Maier, A.G., Przyborski, J., Blatch, G. L. (2011). Intracellular protozoan parasites of humans: the role of molecular chaperones in development and pathogenesis. Protein and Peptide Letters. 15:1117-1125.

Singh, G. P., Chandra, B. R., Bhattacharya, A., Akhouri, R. R., Singh, S. K., and Sharma, A. (2004). Hyper-expansion of asparagines correlates with an abundance of proteins with prion-like domains in *Plasmodium falciparum*. Molecular and Biochemical Parasitology. 137, 307–319

Sijwali, P. S., Rosenthal, P. J. (2010). Functional evaluation of *Plasmodium* export signals in *Plasmodium berghei* suggests multiple modes of protein export. Public Library of Science One. 5: e10227.

Spork, S., Hiss, J. A., Mandel, K., Sommer, M., Kooij, T. W., Chu, T., Schneider, G., Maier, U. G., Przyborski, J. M. (2009). An unusual ERAD-like complex is targeted to the apicoplast of *Plasmodium falciparum*. Eukaryotic Cell. 8: 1134-1145.

Sreerama, N., Venyaminov, S. Y., Woody, R. W. (2000). Estimation of protein secondary structure from circular dichroism spectra: inclusion of denatured proteins with native proteins in the analysis. Analytical Biochemistry. 287: 243-251.

Studier, F.W., Rosenberg, A.H., Dunn, J.J., Dubendorff, J.W. (1990). Use of T7 RNA polymerase to direct expression of cloned genes. Method in Enzymology. 185: 60-89.

Swain, J.F, Dinler, G, Sivendran, R, Montgomery, D. L, Stotz, M, and Gierasch, L. M. (2007). Hsp70 chaperone ligands control domain association via an allosteric mechanism mediated by the interdomain linker. Molecular Cell. 26: 27-39.

Szabo, A., Langer, T., Schroder, H., Flanagan, J., Bukau, B., Hartl, F.U. (1994). A Trimeric Protein Complex Functions as a Synaptic Chaperone Machine. Proceedings of the National Academy of Sciences. USA. 91: 10345-10349.

Thomé, R., Lopes, S.C.P., Costa, F.T.M., Verinaud, L. (2013). Chloroquine: Modes of action of an undervalued drug. Immunology Letters. 153: 50-57.

Thompson, J. K., Rug, M., Cyrklaff, M., Mikkonen, A., Lemgruber, L., Kuelzer, S., Cowman, A. F. (2016). Export of virulence proteins by malaria infected erythrocytes involves remodeling of host actin cytoskeleton. Blood. 124.

Thomsen, T. T., Ishengoma, D. S., Mmbando, B. P., Lusingu, J. P., Vestergaard, L. S., Theander, T. G., Lemnge, M., Bygbjerg, C., Alifrangis, M. (2011). Prevalence of Single Nucleotide Polymorphisms in the *Plasmodium falciparum* Multidrug resistance gene (*Pfmdr-*

1) in Korogwe District in Tanzania before and after introduction of Artemisinin-based combination therapy. American Journal of Tropical Medicine and Hygiene. 85: 979-983.

Trager, W., Jensen, J.B. (1976). Human malaria parasites in continuous culture. Science. 193: 673-675.

Tsai, Y. L., Lee, A. S. (2018). Cell surface GRP78: anchoring and translocation mechanisms and therapeutic potential in cancer: In: Pizzo, S.V. Editor. Cell surface GRP78, a new paradigm in signal transduction biology. Elsevier Inc. 41-62.

Tuteja, R. (2007). Unraveling the components of protein translocation pathway in human malaria parasite *Plasmodium falciparum*. Archives of Biochemistry and Biophysics. 467: 249-260.

Turner, C. T., Russo, V., Santacruz, S., Oram, C., Granville, D. J. (2017). Granzyme B: In: S. Choi. Editor. Encyclopedia of Signaling Molecules.1-7.

Wang, T.F., Chang, J., and Wang, C. (1993). Identification of the peptide binding domain of hsc70 18-Kilo Dalton fragment located immediately after ATPase domain is sufficient for high affinity binding. Journal of Biological Chemistry. 268: 26049-26051.

Wellems, T. E., Plowe, C. V. (2017). Chloroquine-resistant malaria. Journal of Infectious Diseases. 184: 770-6.

WHO (2016). World Health Organisation Global Malaria report; Available on: http://www.who.int/malaria/publications/world-malaria-report-2016/en/

WHO (2018). World Health Organisation Global Malaria report; Available on: http://www.who.int/malaria/world_malaria_report_2018/worldmalariareport2018; accessed on (January 2019).

Whitmore L, Wallace B. A. (2008). Protein secondary structure analyses from circular dichroism spectroscopy: methods and reference databases. Biopolymers. 89: 392-400.

Wittung-Stafshede, P., Guidry, J., Horne, B.E., Landry, S.J. (2003). The J-domain of Hsp40 couples ATP hydrolysis to substrate capture in Hsp70. Biochemistry. 42: 4937-4944.

Zhang, Q., Ma, C., Oberli, A., Zinz, A., Engels, S., Przyborski, J. M. (2017). Proteomic analysis of exported chaperone/co-chaperone complexes of *P. falciparum* reveals an array of complex protein-protein interactions. Nature. 7:42188.

Zhao, T., Zhang, H., Guo, Y., Zhang, Q., Hua, G., Lu, H., Hou, Q., Liu, H., Fan, Z. (2007). Granzyme K cleaves the nucleosome assembly protein SET to induce single-stranded DNA nicks of target cells. Cell Death and Differentiation. 14: 489-499.

Zhu, P., Zhang, D., Chowdhury, D., Martinvalet, D., Keefe, D., Shi, L., Lieberman, J. (2006). Granzyme A, which causes single-stranded DNAdamage, targets the double-strand break repair protein Ku70. European Molecular Biology Organization. 7: 431-7.

Zininga, T., Achilonu, I., Hoppe, H., Prinsloo, E., Dirr, H.W., Shonhai, A. (2016). *Plasmodium falciparum* Hsp70-z, an Hsp110 homologue, exhibits independent chaperone activity and interacts with Hsp70-1 in a nucleotide-dependent fashion. Cell Stress and Chaperone. 21: 499-513

Zininga, T., Shonhai, A. (2014). Are heat shock proteins druggable candidates? American Journal of Biochemistry and Biotechnology. 10: 211-213.

Zininga, T., Makumire, S., Gitau, G. W., Njunge, J. M., Pooe, O. J., Klimek, H., Scheurr, R., Raifer, H., Prinsloo, E., Przyborski, J.M., Hoppe, H., and Shonhai, A. (2015). *Plasmodium falciparum* Hop (PfHop) interacts with the Hsp70 chaperone in a nucleotide-dependent fashion and exhibits ligand Selectivity. Public Library of Science One. 10: e0135326.

Zininga, T. (2015). Characterization of heat shock protein 70-z (PfHsp70-z) from *Plasmodium falciparium* (Doctoral dissertation). Available http://univendspace.univen.ac.za/handle/11602/619. (Accessed October 2017).

Zininga, T., Achilonu, I., Hoppe, H., Prinsloo, E., Dirr, H.W., and Shonhai, A. (2015). Overexpression, purification and characterisation of the *Plasmodium falciparum* Hsp70-z (PfHsp70-z) protein. Public Library of Science One. 10: e0129445.

Zininga T., Ramatsui L., Makhado P., Makumire S., Achilinou I., Hoppe H., Dirr H., Shonhai A. (2017b). (−)-Epigallocatechin-3-gallate inhibits the chaperone activity of *Plasmodium falciparum* Hsp70 chaperones and abrogates their association with functional partners. Molecules. 22: 2139.

Zininga, T., Pooe O., Makhado P., Ramatsui L., Prinsloo E., Achilonu I., Dirr H., Shonhai A. (2017a). Polymyxin B inhibits the chaperone activity of *Plasmodium falciparum* Hsp70. Cell Stress and Chaperones. 22: 707-715.

Zügel, U., and Kaufman, S.H.E. (1999). Role of heat shock proteins in protection from and pathogenesis of infectious disease. Journal of Clinical Microbiology. 12: 19-39.

Appendices

Appendix A: Methodology

A.1. Preparation of *E. coli* BL21 (DE3) competent cells

The competent cells were prepared following growth overnight at 37 °C on double strength (2 x YT) agar plates (1.6 % w/v Tryptone, 1 % w/v Yeast extract, 0.5 % w/v NaCl, 1.5 % w/v) and autoclaved at 121 °C for 15 minutes with no addition of antibiotics. A single colony was picked and inoculated into 5 ml of 2 x YT broth and grown overnight at 37 °C. The overnight culture was transferred into fresh 2 x YT broth (1: 200) and grown to OD_{600} = 0.4-0.6. The culture was then be centrifuged for 10 minutes at 5000 g at 4 °C. The supernatant was discarded and 0.1 M $MgCl_2$ was added to the pallet. The pallet was resuspended and incubated on ice for 30 minutes. The suspension was then centrifuged at 5000 g for 10 minutes at 4 °C and the supernatant was discarded. The remaining pellet was re-suspended in 0.1 M $CaCl_2$ and incubated on ice for 4 hours. This was followed by centrifugation and discarding of the supernatant. Prior to storage equal amounts 0.1 M of $CaCl_2$ and 30 % glycerol was added and allowed to incubate on ice for the mixture to dissolve. The cell suspension was then aliquoted (200 µl per tube) into pre-chilled 2 ml tubes and stored at -80 °C.

A.2. Transformation of plasmids into competent cells and DNA extraction

The constructs pQE30/PfHsp70-x, pQE30/PfHsp70-xT and pQE30/hHsp70 plasmid were transformed into *E. coli* BL21 (DE3) cells. Plasmid DNA (2 ng) was added into an aliquoted 100 µl of competent cells. The cells were then incubated on ice for 30 minutes followed by heat shocking at 42 °C for 45 seconds and immediately placed on ice for 10 minutes. The tubes were then topped up with 900 µl of 2x YT broth and incubated at 37 °C for 1 hour. The cells were then streaked onto 2x YT plates containing the desired antibiotics and allowed to grow at 37 °C overnight.

DNA extraction was done using a Zippy plasmid Miniprep kit as per manufacturer's instructions (Zymo research, USA).

Table A.1. Restriction digest reaction mixture

	Tube 1 (control)	Tube 2 (*Bam* HI)	Tube 3 (*Hind* III)	Tube 4 (both *Bam* HI and *Hind* III)
H2O	16 µL	15 µL	14 µL	13 µL
Buffer	2 µL	2 µL	2 µL	2 µL
DNA	2 ng	2 ng	2 ng	2 ng
Enzyme	-	1 µL	2 µL	3 µL
Total	20 µL	20 µL	20 µL	20 µL

A.3. SDS-PAGE analysis of proteins

The PfHsp70-xF, PfHsp70-xT and hHsp70 proteins were treated by boiling in SDS sample buffer (0.25 % Coomasie Brilliant blue (R250); 2 % SDS; 10 % glycerol (v/v); 100 mM Tris; 1 % β-mercaptoethanol) in a ratio of 4:1 for 10 minutes at 95 °C and resolved using 12 % acrylamide resolving gel. The gels were then transferred into the electrophoresis tank and electrophoresis buffer (25 mM Tris-HCl, pH 8.3, 250 mM glycine and 0.1 % (w/v) SDS) was added. The boiled samples were loaded in respective wells and pre-stained protein molecular weight markers (ThermoFisher Scientific, USA) were also loaded. The electrophoresis was performed at 100 volts for 1 hour-20 minutes using the Bio-Rad Mini protein 3 electrophoresis system (BioRad, USA). The running gel and stacking gel for SDS-PAGE analysis of both proteins were prepared as in table A.2 and A.3.

Table A.2. SDS-PAGE running gel preparation

Reagents	X 1
Bis	30 % (w/v)
Tris pH 8.8	1.5 M
SDS	10 % (w/v)
H_2O	1.58 ml
APS	10 % (w/v)
TEMED	20 µL

Table. A.3. SDS-PAGE stacking gel preparation

Reagents	X 1
Bis	30 % (w/v)
Tris pH 6.8	0.5 M
SDS	10 % (w/v)
H_2O	1.05 ml
APS	10 % (w/v)
TEMED	20 µL

A.4. Western blot analysis of proteins

On completion of electrophoresis, SDS-PAGE gels were removed from glass plates and the stacking gel cut off. The resolving gel, nitrocellulose membrane, 3 mm Whatman filter papers and two dry blots were immersed in ice cold Western transfer buffer (25 mM Tris; 192 mM glycine, 20 % methanol) to equilibrate for about 15 minutes. The gel was then placed on the filter paper on top of the dry blot. The nitrocellulose paper was then laid over the gel, followed by the filter paper and the other dry blot. The transfer was run at 100 volts for 8 minutes.

A.5. Protein quantification

Protein concentration were determined by Bradford's method (Bradford, 1976). BSA standards were prepared with concentrations ranging from 0 to 1 mg/ml in 0.15 M PBS (137 mM NaCl, 27 mM KCL, 4.3 mM Na_2HPO_4 and 1.4 mM KH_2PO_4). Bradford's reagent (250 µl) (10 % Coomassie G250 in 95 % ethanol, 85 % (w/v) phosphoric acid) was added to 5 µl of protein and the reaction incubated at room temperature for 5 minutes. Absorbance was read at 595 nm. The protein eluents (5 µl) were treated similarly and the protein concentrations were determined by extrapolation from the standard curve.

Appendix B: Supplementary data

B1: Bradford's assay

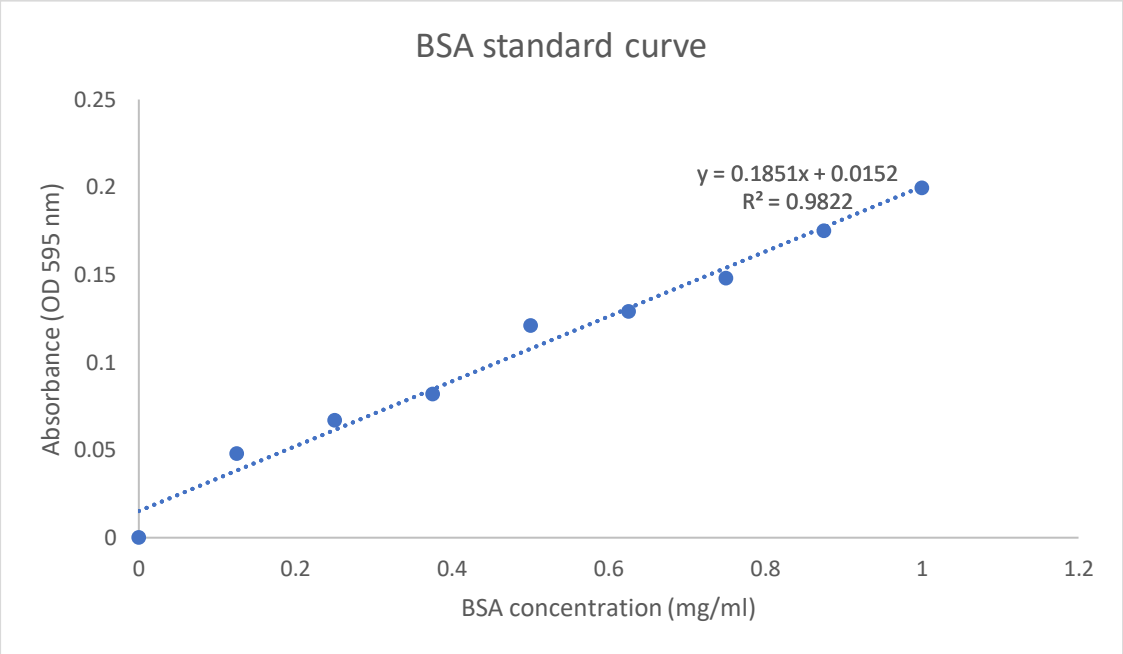

Figure B.1. Protein quantification standard curve
The PfHsp70-xF, PfHsp70-xT and hHsp70 protein concentrations were determined using Bradford's reagent. The R^2 value of the standard curve was 0.9822 and the equation was y=0.1851x+0.0152.

B.2. Analysis of the secondary structure of the Hsp70s

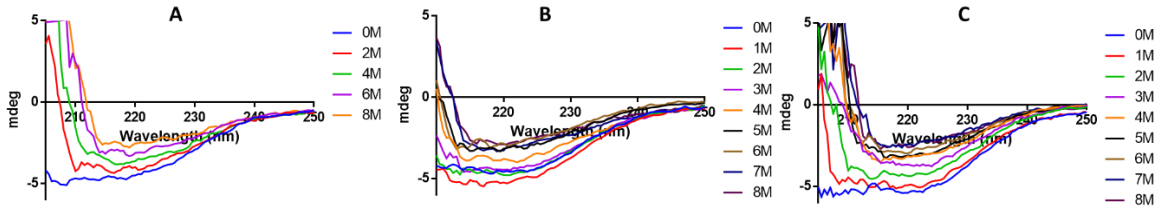

Figure B.2. The effect of urea on the secondary structure analyses using CD spectroscopy
The effect of varying concentrations of urea on the secondary structure of A. PfHsp70-xF, B. PfHsp70-xT and C. hHsp70 proteins.

B.3. Interaction of PfHsp70-xF, PfHsp70-xT and hHsp70 with GrB are concentration dependent

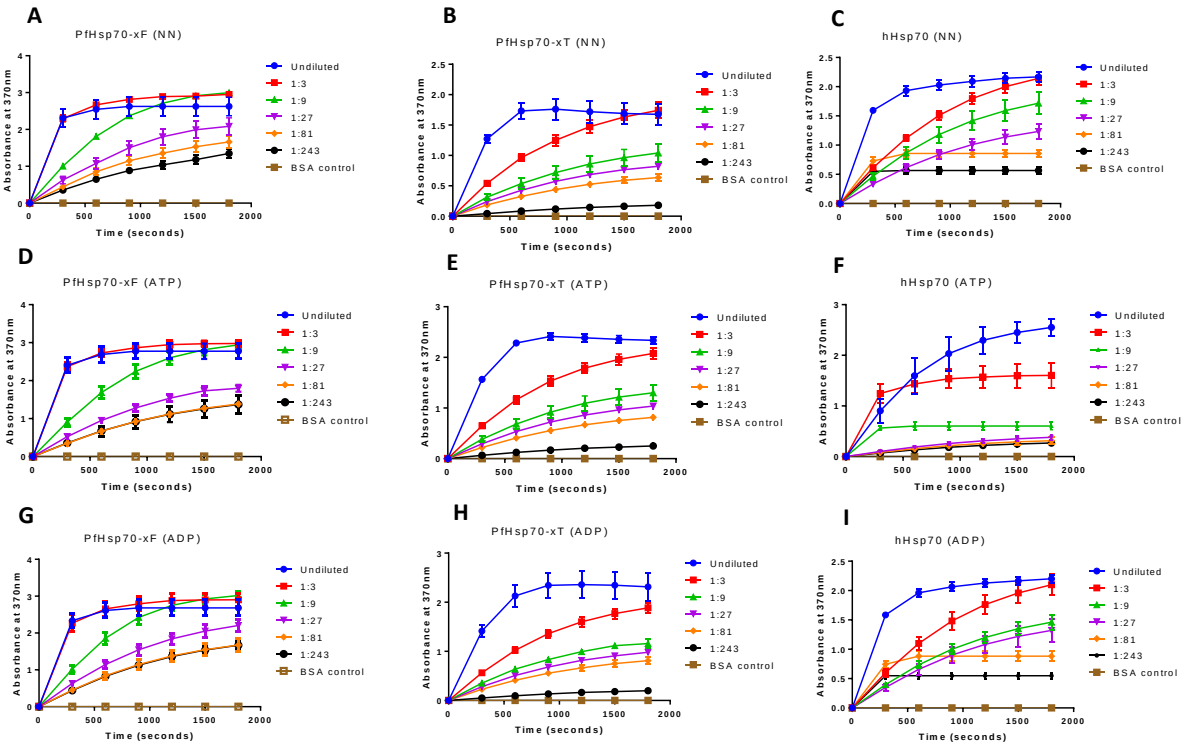

Figure B.3. The interactions of PfHsp70-xF/PfHsp70-xT and hHsp70 with GrB are concentration dependent. The representative interaction curves generated from the ELISA analysis of the association of GrB with PfHsp70-xF (A), PfHsp70-xT-GrB (B) and hHsp70-GrB (C). The assay was conducted in the presence of varying amounts of GrB towards establishing dose-dependent association. The assay was repeated in presence of 5 mM ATP for PfHsp70-xF-GrB association (D), PfHsp70-xT-GrB association (E) and hHsp70-GrB (F); and in the presence of 5 mM ADP for PfHsp70-xF-GrB association (G), PfHsp70-xT-GrB association (H) and hHsp70-GrB (I), respectively. The error bars represent the SDs obtained about the means of at least three assays conducted using independently purified recombinant protein batches.

Appendix C: Materials

Table C.1. List of reagents used

Reagent	Supplier
Acetic acid	Merck, Germany
Adenosine triphosphate (ATP)	Sigma-Aldrich, USA
Agarose	Merck, Germany
Ammonium persulphate	Sigma-Aldrich, USA
Ampicillin	Melford, UK
Bovine serum albumin	Melford, UK
Bromophenol blue	Merck, Germany
Calcium chloride	Merck, Germany
Chemiluminescence Western blotting kit	Amersham, USA
Nitrocellulose membrane	Thermo Scientific, USA
Immobilon®-P transfer Membrane	Merck, Germany
Coomasie brilliant blue R250	Merck, Germany
Ethidium bromide	Merck, Germany
Glacial acetic acid	Merck, Germany
Glycerol	Merck, Germany
Glycine	Merck, Germany
Glucose	Merck, Germany
Imidazole	Merck, Germany
Isopropyl-1-thio-D-galacopyranoside	Sigma-Aldrich, USA
GeneRuler 1 Kb DNA ladder	Thermo Scientific, USA
Lysozyme	Merck, Germany
Magnesium chloride	Merck, Germany
Methanol	Merck, Germany
Phenylmethylsufonyl fluoride	Merck, Germany
Polyacrylamide	Merck, Germany
Ponceau S	Sigma-Aldrich, USA
Amicon® Ultra-15 10K centrifuge filter device	Merck, Germany
Sodium chloride	Merck, Germany
Sodium dodecyl sulphate	Merck, Germany
Sodium hydroxide	Merck, Germany
TEMED	Sigma-Aldrich, USA
Tris-HCl	Merck, Germany
Tryptone	Oxoid, England
Tween 20	Melford, UK
Yeast	Merck, Germany
Page ruler prestained protein ladder	Thermo Scientific, USA
Nutrient agar	Merck, Germany